

---

# First-ish Order Methods: Hessian-aware Scalings of Gradient Descent

---

Oscar Smee<sup>1</sup> Fred Roosta<sup>1,2</sup> Stephen J. Wright<sup>3</sup>

## Abstract

Gradient descent is the primary workhorse for optimizing large-scale problems in machine learning. However, its performance is highly sensitive to the choice of the learning rate. A key limitation of gradient descent is its lack of natural scaling, which often necessitates expensive line searches or heuristic tuning to determine an appropriate step size. In this paper, we address this limitation by incorporating Hessian information to scale the gradient direction. By accounting for the curvature of the function along the gradient, our adaptive, Hessian-aware scaling method ensures a local unit step size guarantee, even in nonconvex settings. Near a local minimum that satisfies the second-order sufficient conditions, our approach achieves linear convergence with a unit step size. We show that our method converges globally under a significantly weaker version of the standard Lipschitz gradient smoothness assumption. Even when Hessian information is inexact, the local unit step size guarantee and global convergence properties remain valid under mild conditions. Finally, we validate our theoretical results empirically on a range of convex and nonconvex machine learning tasks, showcasing the effectiveness of the approach.

## 1. Introduction

Consider the optimization problem

$$\min_{\mathbf{x} \in \mathbb{R}^d} f(\mathbf{x}), \quad (1)$$

where  $f : \mathbb{R}^d \rightarrow \mathbb{R}$  is twice continuously differentiable, bounded below, and possibly nonconvex. Arguably, the simplest and most widely used workhorse for solving such

<sup>1</sup>School of Mathematics and Physics, University of Queensland, Brisbane Australia. <sup>2</sup>ARC Training Centre for Information Resilience (CIRES), Brisbane, Australia <sup>3</sup>Computer Sciences Department, University of Wisconsin-Madison, USA. Correspondence to: Oscar Smee <o.smee@uq.edu.au>.

problems in large-scale machine learning is gradient descent (GD) and its stochastic variants (Lan, 2020). Recall that an iteration of GD takes the form

$$\mathbf{x}_{k+1} = \mathbf{x}_k - \alpha_k \mathbf{g}_k,$$

where  $\mathbf{g}_k \triangleq \mathbf{g}(\mathbf{x}_k) = \nabla f(\mathbf{x}_k)$  is the gradient of  $f$  at  $\mathbf{x}_k$ .

Gradient descent is favored for its simplicity, low per-iteration cost, and convergence properties in nonconvex settings. With an arbitrary initialization  $\mathbf{x}_0$ , the only hyperparameter is the step size,  $\alpha$ , which may vary across iterations. Choosing this parameter has been the focus of significant research. Most analyses assume Lipschitz smoothness of the gradient, equivalent to a uniform upper bound on the Hessian spectrum for twice continuously differentiable functions. However, this approach often ignores *local* curvature, leading to conservative step sizes. Additionally, since the gradient’s Lipschitz constant is typically unknown, the step size is often determined through backtracking line search, without an a priori known effective initialization, or via simple trial and error, significantly increasing computational overhead.

In contrast to first-order methods, most second-order methods incorporate local curvature information to construct properly scaled directions, ensuring that a unit step size ( $\alpha = 1$ ) achieves a sufficient decrease in the function value<sup>1</sup> near a local solution (Boyd & Vandenberghe, 2004; Nocedal & Wright, 2006). This property allows  $\alpha = 1$  to serve as an initial guess in backtracking line search, as it will eventually meet the acceptance criteria. By leveraging local curvature, second-order methods often converge in significantly fewer iterations than first-order methods (Martens, 2010). However, this advantage comes at the cost of higher per-iteration computational expense.

These facts lead us to the motivating question for our paper: *Can local curvature information be used to properly, and efficiently, scale the gradient—without altering its direction—to attain certain desirable properties of both first and second-order methods?* To that end, we propose our “first-ish order”

<sup>1</sup>This brings to mind the following quote about the significance of a unit step size: “Any optimization algorithm for which the unit step length works has some wisdom. It is too much of a fluke if the unit step length [accidentally] works.” - J. Nocedal (Source.)

method, which employs updates of the form:

$$\mathbf{x}_{k+1} = \mathbf{x}_k + \alpha_k \mathbf{p}_k, \quad \mathbf{p}_k = -s_k \mathbf{g}_k, \quad (2)$$

where  $s_k > 0$  is an adaptive, *Hessian-aware* scaling and  $\alpha_k > 0$  is the step size, chosen to ensure global convergence. We distinguish between  $s_k$  and  $\alpha_k$  to emphasize that the scaling is applied, prior to, and independently of, the step size selection strategy (e.g., line search).

Remarkably, we show that certain Hessian-aware scalings, which can be calculated using only a single Hessian-vector product, can endow GD with a property typically restricted to second-order methods, namely, a local unit step size guarantee. The key to our results is the fact that the scaled gradient direction,  $\mathbf{p}_k$ , satisfies the following *second-order descent condition*<sup>2</sup>:

$$\langle \mathbf{g}_k, \mathbf{p}_k \rangle + \langle \mathbf{p}_k, \mathbf{H}_k \mathbf{p}_k \rangle \leq 0, \quad (3)$$

where  $\mathbf{H}_k \triangleq \mathbf{H}(\mathbf{x}_k) = \nabla^2 f(\mathbf{x}_k)$  is the Hessian of  $f$  at  $\mathbf{x}_k$ . This property (3) is typically satisfied by search directions in second-order methods. When there is positive curvature along  $\mathbf{p}$ , (3) strengthens the standard first-order descent condition  $\langle \mathbf{g}, \mathbf{p} \rangle < 0$ . For instance, the Newton direction  $\mathbf{p}_N = -\mathbf{H}^{-1} \mathbf{g}$ , as well as directions produced by inexact methods like Newton-MR and Newton-CG, satisfy (3) as long as a non-positive curvature (NPC) is not detected (see, e.g., (Liu & Roosta, 2022, Lemma 13) and (Nocedal & Wright, 2006, Chapter 5)).

The descent condition (3) eliminates the need to bound curvature terms, enabling the use of analytical tools typically associated with second-order methods, without prior knowledge of problem constants. Our key upper bound (see (14)) incorporates local curvature information and is derived from Lipschitz Hessian smoothness (Assumption 3.1), despite the step *direction* relying solely on first-order information.

**Contributions.** Our contributions are outlined as follows:

1. In Section 3.1, we show that, when the gradient is small, the Armijo line search applied to the rescaled gradient direction will accept a unit step size, even for nonconvex  $f$ . We establish global convergence under relaxed smoothness conditions, which generalize Lipschitz continuity of the gradient and Hessian.
2. In Section 3.2, we analyze the local convergence properties of our method. We show that near a minimum, under certain conditions, the unit step size is accepted at each iteration, leading to local linear convergence of the function value with a rate that may improve upon typical local gradient descent rates. For a specific scaling, we

<sup>2</sup>Note that (3) has also been called “2.5<sup>th</sup> order descent” as it is a stronger condition than the typical reduction in the local quadratic approximation to the objective.

also establish local linear convergence in the gradient norm.

3. In Section 3.3, we examine the case in which the Hessian is inexact. Under certain conditions on the inexactness, we show that a unit step size and global convergence guarantee similar to the exact case applies.
4. Finally, in Section 4, we validate our results numerically on large scale, nonconvex objectives arising from problems in data science.

## 2. Our Approach

We now introduce and motivate our Hessian-aware scalings and highlight their key properties.

### 2.1. Hessian-aware Scaling

To determine the scaling  $s_k$  in (2) required for the update direction,  $\mathbf{p}_k$ , to achieve *natural scaling* (i.e., eventual unit step length), we draw inspiration from the Newton’s method in one dimension. We also account for varying curvature along the gradient direction, considering cases of strongly positive, limited positive, and negative curvature.

**Strong Positive Curvature (SPC).** For strongly convex problems, the Newton direction minimizes the local quadratic approximation:  $\min_{\mathbf{p}} \langle \mathbf{p}, \mathbf{g} \rangle + \langle \mathbf{p}, \mathbf{H} \mathbf{p} \rangle / 2$ . Restricting to  $\mathbf{p} = -s \mathbf{g}$ , and assuming  $\langle \mathbf{g}, \mathbf{H} \mathbf{g} \rangle > 0$ , the optimal scaling is given by

$$s^{\text{CG}} = \frac{\|\mathbf{g}\|^2}{\langle \mathbf{g}, \mathbf{H} \mathbf{g} \rangle}. \quad (4)$$

The notation  $s^{\text{CG}}$  reflects a connection to the conjugate gradient (CG) method, discussed in Section 2.3. An alternative motivation for Newton’s method is solving the optimization problem  $\min_{\mathbf{p}} \|\mathbf{H} \mathbf{p} + \mathbf{g}\|^2$ . By restricting the search to  $\mathbf{p} = -s \mathbf{g}$ , the unique minimizing scaling is given by

$$s^{\text{MR}} = \frac{\langle \mathbf{g}, \mathbf{H} \mathbf{g} \rangle}{\|\mathbf{H} \mathbf{g}\|^2}. \quad (5)$$

The notation  $s^{\text{MR}}$  highlights a connection to the minimum residual (MINRES) method, as discussed in Section 2.3.

From these two fundamental scalings, additional factors like the geometric mean of CG and MR scalings can be derived:

$$s^{\text{GM}} = \sqrt{s^{\text{MR}} s^{\text{CG}}} = \frac{\|\mathbf{g}\|}{\|\mathbf{H} \mathbf{g}\|}. \quad (6)$$

The CG, GM, and MR scalings each reflect an aspect of the inverse Hessian restricted to one dimension. For example, the CG scaling in (4) is an inverse Rayleigh quotient of the Hessian,  $\mathbf{H}$ , with respect to  $\mathbf{g}$ , while the MR scaling in (5)

corresponds to a Rayleigh quotient of the Hessian pseudo-inverse,  $\mathbf{H}^\dagger$ , with respect to  $\mathbf{H}\mathbf{g}$  (using  $\mathbf{H}\mathbf{H}^\dagger\mathbf{H} = \mathbf{H}$ ). In the univariate case, all scalings reduce to the inverse of the second derivative, making the update in (2) the exact Newton step. Thus, these scalings are most effective under SPC along the gradient direction, i.e.,  $\langle \mathbf{g}, \mathbf{H}\mathbf{g} \rangle > \sigma \|\mathbf{g}\|^2$  for some  $\sigma > 0$ . The SPC condition can be interpreted as a strong convexity condition *restricted to the gradient direction*.

**Negative Curvature (NC).** In nonconvex settings, the indefiniteness of the Hessian can make the gradient a NC direction, i.e.,  $\langle \mathbf{g}, \mathbf{H}\mathbf{g} \rangle < 0$ . Since  $-\mathbf{g}$  is already a descent direction, both the first and second directional derivatives along  $-\mathbf{g}$  are negative, regardless of scaling choice. Previous theoretical results (Gould et al., 2000; Curtis & Robinson, 2019; Liu & Roosta, 2022) and practical experience suggest that substantial progress can be made with large steps along negative curvature directions.

**Limited Positive Curvature (LPC).** The LPC case, where  $0 \leq \langle \mathbf{g}, \mathbf{H}\mathbf{g} \rangle \leq \sigma \|\mathbf{g}\|^2$ , represents a middle ground between SPC and NC, characterized by small but non-negative curvature along  $\mathbf{g}$ . Here,  $\sigma$  acts as a gradient Lipschitz constant, constraining the second-order term in the Taylor expansion along  $-\mathbf{g}$ . Since second-order information is unreliable in this regime, we revert to gradient descent with a step size independent of second-order information. Thanks to the curvature bound  $\sigma$ , scalings satisfying  $s \leq 1/\sigma$  maintain second-order descent properties akin to those in the SPC and NC cases.

The above discussions are summarized in Algorithm 1.

---

**Algorithm 1** Hessian-aware Scaling Selection
 

---

- 1: **Inputs:** Gradient  $\mathbf{g}$ , Hessian  $\mathbf{H}$ , and SPC scaling tolerance  $\sigma > 0$ .
  - 2: Set the range for LPC scaling as  $s_{\min}^{\text{LPC}} \in (0, 1/\sigma)$ .
  - 3: Set the range for NC scaling as  $0 < s_{\min}^{\text{NC}} \leq s_{\max}^{\text{NC}} < \infty$ .
  - 4: **if**  $\langle \mathbf{g}, \mathbf{H}\mathbf{g} \rangle > \sigma \|\mathbf{g}\|^2$  **then**
  - 5:   choose  $s^{\text{SPC}} \in \{s^{\text{MR}}, s^{\text{CG}}, s^{\text{GM}}\}$ , set  $\mathbf{p} = -s^{\text{SPC}}\mathbf{g}$ , set FLAG = SPC.
  - 6: **else if**  $0 \leq \langle \mathbf{g}, \mathbf{H}\mathbf{g} \rangle \leq \sigma \|\mathbf{g}\|^2$  **then**
  - 7:   choose  $s^{\text{LPC}} \in [s_{\min}^{\text{LPC}}, 1/\sigma]$ , set  $\mathbf{p} = -s^{\text{LPC}}\mathbf{g}$ , set FLAG = LPC.
  - 8: **else**
  - 9:   choose  $s^{\text{NC}} \in [s_{\min}^{\text{NC}}, s_{\max}^{\text{NC}}]$ , set  $\mathbf{p} = -s^{\text{NC}}\mathbf{g}$ , set FLAG = NC.
  - 10: **end if**
  - 11: **Return**  $\mathbf{p}$ , FLAG.
- 

As shown in Proposition 2.2, the constant  $1/\sigma$  bounds the

step size in both the SPC and LPC cases, so  $\sigma$  should generally be chosen small ( $\sigma \ll 1$ ). For fixed steps,  $s_{\min}^{\text{LPC}}$  can be set to  $1/\sigma$ , and  $s_{\min}^{\text{NC}} = s_{\max}^{\text{NC}}$ . While  $s_{\max}^{\text{NC}}$  theoretically allows large scalings due to negative curvature, in practice it can also be set to  $1/\sigma$ .

*Remark 2.1.* Computationally, Algorithm 1 requires an additional Hessian-vector product,  $\mathbf{H}\mathbf{g}$ , for curvature testing and scaling computation. This product can be efficiently evaluated without computing the full Hessian, using techniques like automatic differentiation (Pearlmutter, 1994; Baydin et al., 2018), which requires only an extra forward and backward pass through the computational graph. Although this incurs additional cost, our numerical experiments show that scaled gradient descent can have lower overall computational costs compared to alternatives, as it eliminates the need for multiple backtracking line search evaluations or trial-and-error step size selection. This efficiency stems from the local unit step size guarantee (see Proposition 3.2), avoiding costly function evaluations during line search.

## 2.2. Basic Properties

We collect some basic properties of the scalings from Algorithm 1. We relegate all proofs to Appendix A.

**Proposition 2.2** (Scaling Upper Bounds). *In the SPC case,  $0 < s^{\text{MR}} \leq s^{\text{GM}} \leq s^{\text{CG}} \leq 1/\sigma$ , while for the LPC case,  $0 < s^{\text{LPC}} \leq 1/\sigma$ . Finally, in the NC case,  $0 < s^{\text{NC}} \leq s_{\max}^{\text{NC}}$ .*

The proof of this result demonstrates the importance of verifying strong positive curvature, in order to obtain an upper bound in the SPC and LPC cases.

**Proposition 2.3** (Second-order Descent). *Suppose  $\mathbf{g} \neq 0$ . The direction  $\mathbf{p}$  returned by Algorithm 1 satisfies both the first-order descent condition  $\langle \mathbf{g}, \mathbf{p} \rangle < 0$  and the second-order descent condition (3).*

*Remark 2.4.* Our selection of scalings satisfying second-order descent is not exhaustive. For instance, if  $f$  has an  $L_{\mathbf{g}}$ -Lipschitz gradient,  $s = 1/L_{\mathbf{g}}$  ensures (3) by conservatively controlling curvature. However, this choice is not adaptive to local curvature, and  $L_{\mathbf{g}}$  may be unknown.

A well-known property of classical Newton’s method is its invariance under affine transformations (Boyd & Vandenberghe, 2004, Chapter 9.5). While directions parallel to gradient cannot achieve full affine invariance for general objectives, Proposition 2.5 shows that our Hessian-aware scalings lead to invariance to scalar transformations.

**Proposition 2.5** (Scalar Invariance). *Consider (2) with  $s_k = s_k^{\text{SPC}}$  for all  $k$ , applied to  $f(\mathbf{x})$  and its scalar reparameterization  $f(\mathbf{y})$  where  $\mathbf{y} = \mathbf{x}/c$  for any  $c \neq 0$ . Then  $\mathbf{y}_k = \mathbf{x}_k/c$  for all  $k$ .*

Although understandably limited compared to the full affine invariance of Newton’s method, this invariance property

distinguishes our approach from standard gradient descent, where the step size is highly sensitive to changes in the coordinate system.

### 2.3. Related Works

**Quadratic Problems.** The scalings (4) and (5) are well-studied for strongly convex quadratic functions; see (Gonzaga & Schneider, 2016; MacDonald et al., 2024) and references therein. These correspond to exact line search methods along the gradient direction for  $f$  and  $\|\mathbf{g}\|^2$ , known as steepest descent and minimal gradient methods, respectively<sup>3</sup>. The GM scaling (6) has been studied for such problems by (Dai & Yang, 2006), showing that for  $\alpha > 0$ ,  $s^{\text{GM}}$  estimates an inverse gradient Lipschitz constant.

**Barzilai-Borwein Methods.** The Barzilai-Borwein (BB) method (Barzilai & Borwein, 1988; Fletcher, 2005; Dai et al., 2019) is also based on scalar minimization of a second-order approximation. For quadratics, the long and short BB step sizes align with our CG and MR scalings, shifted by one iteration, due to their equivalence to steepest descent and minimal gradient methods. While BB achieves R-linear convergence for strongly convex quadratics, its convergence for non-quadratic objectives cannot be guaranteed.

**Inexact Newton Methods.** The scalings  $s^{\text{CG}}$  and  $s^{\text{MR}}$  are deeply connected to Krylov subspace-based inexact Newton methods. The Newton-CG method (Nocedal & Wright, 2006) uses CG to solve the Newton system. The  $t^{\text{th}}$  iteration of CG amounts to solving

$$\min_{\mathbf{d} \in \mathcal{K}_t(\mathbf{H}, \mathbf{g})} \frac{1}{2} \langle \mathbf{d}, \mathbf{H}\mathbf{d} \rangle + \langle \mathbf{g}, \mathbf{d} \rangle,$$

where  $\mathcal{K}_t(\mathbf{H}, \mathbf{g}) = \text{Span}\{\mathbf{g}, \mathbf{H}\mathbf{g}, \dots, \mathbf{H}^{t-1}\mathbf{g}\}$  is the Krylov subspace of degree  $t$ . For  $t = 1$ ,  $\mathcal{K}_1(\mathbf{H}, \mathbf{g}) = \{s\mathbf{g} : s \in \mathbb{R}\}$ , and the solution is  $-s^{\text{CG}}\mathbf{g}$ . Similarly, the Newton-MR method (Roosta et al., 2022; Liu & Roosta, 2022; Smeë & Roosta, 2024; Lim & Roosta, 2023), based on MINRES (Paige & Saunders, 1975), computes the approximate Newton direction as a solution to

$$\min_{\mathbf{d} \in \mathcal{K}_t(\mathbf{H}, \mathbf{g})} \|\mathbf{H}\mathbf{d} + \mathbf{g}\|,$$

yielding  $-s^{\text{MR}}\mathbf{g}$  for  $t = 1$ . These connections to inexact second-order methods motivated the study of CG and MR scaled gradient methods. The treatment of limited positive curvature in (Smeë & Roosta, 2024; Lim & Roosta, 2023) inspired our curvature validation procedure.

**Smoothness and Adaptivity.** The global convergence analysis in this paper does not rely on the conventional

<sup>3</sup>Beyond quadratics, there is no correspondence to exact line search, so we avoid labeling (4) and (5) as such.

Lipschitz gradient smoothness assumption, which has come under increasing scrutiny in recent works. Many machine learning objectives, such as feedforward or recurrent neural networks, fail to satisfy this condition (Patel et al., 2022). Recent studies suggest that this assumption may not hold even along the optimization trajectory (Cohen et al., 2021). Instead, Ahn et al. (2022, Remark 5) argue that *Lipschitz Hessian smoothness* is more appropriate; our work adopts a weaker form of this assumption (Assumption 3.3). Additionally, Patel & Berahas (2024) study gradient descent with diminishing step sizes under local Lipschitz smoothness, a weaker assumption than the standard one.

Our method avoids globally conservative step sizes, instead using adaptive local curvature information to guide step size selection. Recent studies suggest that conservative step sizes can hinder convergence. Grimmer (2024) show that larger step sizes can improve rates, while Altschuler & Parrilo (2024) demonstrate that combining long and short steps enhances convergence in convex settings. Dynamic step size selection incorporates local information, e.g., the Polyak step size (Polyak, 1987) and its variants (Loizou et al., 2021; Orvieto et al., 2022; Oikonomou & Loizou, 2024). Malitsky & Mishchenko (2020; 2024) adaptively set step sizes using local Lipschitz estimates and control sequences, ensuring global convergence under convexity and locally Lipschitz gradients. Mishkin et al. (2024) explores adaptive step sizes via directional smoothness, closely related to our use of gradient curvature. Berahas et al. (2024) investigates local first-order smoothness oracles, while methods like D-adaptation (Defazio & Mishchenko, 2023; Mishchenko & Defazio, 2024) and Do(W)G (Ivgi et al., 2023; Khaled et al., 2023) achieve parameter-free convergence by adaptively estimating problem constants.

**Quadratic Model Scaling** Utilizing a quadratic model to rescale search directions is not new. The KFAC method (Martens & Grosse, 2015) rescales directions using a quadratic model based on the Fisher information matrix. Similarly, Roulet et al. (2024) adaptively set the step size using a quadratic model of the objective along a search direction, akin to our CG scaling. Roulet et al. (2024) show that curvature-aware scaling can align optimization dynamics with the edge of stability (Cohen et al., 2021), though they do not exploit negative curvature or provide theoretical guarantees. Castera et al. (2022) use a quadratic model (similar to our CG scaling) to verify curvature, enabling BB step sizes in nonconvex and stochastic settings, and also find that large step sizes are viable with negative curvature. de Gournay & Gossard (2022) rescale step directions using directional second-order information, applying a moving average of directional curvatures, but focus on practical implementation without convergence theory.

### 3. Convergence Analyses

In Section 3.1, we consider the global properties of (2) with Algorithm 1 and the classical Armijo line-search strategy. In Section 3.2, we consider the local convergence properties. Finally, in Section 3.3, we investigate the case of inexact Hessian. We defer all proofs to Appendix B.

#### 3.1. Global Convergence

To globalize the iteration in (2), we select a step size via the Armijo condition, which requires  $\alpha$  to satisfy

$$f(\mathbf{x} + \alpha \mathbf{p}) \leq f(\mathbf{x}) + \rho \alpha \langle \mathbf{p}, \mathbf{g} \rangle, \quad (7)$$

for some constant  $\rho \in (0, 1/2)$ . The resulting method is depicted in Algorithm 2, where backtracking (Algorithm 3 in Appendix B.1) and forward tracking (Algorithm 4 in Appendix B.1) strategies are used to find  $\alpha_k$  satisfying (7).

---

#### Algorithm 2 Scaled Gradient Descent With Line Search

---

- 1: **Input:** Line search parameter  $\rho < 1/2$ , termination tolerance  $\varepsilon_g > 0$ .
  - 2: **while**  $\|\mathbf{g}_k\| \geq \varepsilon_g$  **do**
  - 3:    $[\mathbf{p}_k, \text{FLAG}] \leftarrow$  Call Algorithm 1 with  $\mathbf{H}_k$ ,  $\mathbf{g}_k$  and  $\sigma$
  - 4:   For  $\text{FLAG} = \text{SPC/LPC}$ , use Algorithm 3 to find  $\alpha_k \in (0, 1]$  satisfying (7). For  $\text{FLAG} = \text{NC}$ , use Algorithm 4 to find  $\alpha_k \in (0, \infty)$  satisfying (7).
  - 5:    $\mathbf{x}_{k+1} = \mathbf{x}_k + \alpha_k \mathbf{p}_k$
  - 6: **end while**
- 

Our analysis relies on a weakened version of the typical Lipschitz Hessian smoothness condition, requiring smoothness to hold only along the negative-gradient direction.

**Assumption 3.1** (Hessian Directional Smoothness). There exists,  $0 \leq L_2 < \infty$  such that,  $\forall \mathbf{x} \in \mathbb{R}^d$  and  $\forall t \geq 0$

$$\|\mathbf{H}(\mathbf{x} - t\mathbf{g}(\mathbf{x})) - \mathbf{H}(\mathbf{x})\| \leq tL_2 \|\mathbf{g}(\mathbf{x})\|. \quad (8)$$

While Assumption 3.1 may be difficult to verify directly, it is implied by Hessian Lipschitz continuity. If  $f$  satisfies the latter with constant  $L_H$ , then  $L_2 \leq L_H$ . However,  $L_2$  can be much smaller than  $L_H$ , as Assumption 3.1 applies only along a single direction at each  $\mathbf{x}$ .

The following result states that, local to a critical point, the unit step size  $\alpha = 1$  ensures sufficient decrease for the scaled gradient direction,  $\mathbf{p}$ .

**Proposition 3.2** (Sufficient Condition for Acceptance of Unit Step Size). *Consider Assumption 3.1 and let  $\mathbf{p}$  be the direction selected by Algorithm 1. The Armijo line search (7) is satisfied with  $\alpha = 1$  if*

$$\|\mathbf{g}\| \leq \min \left\{ \frac{6\sigma^2(1/2 - \rho)}{L_2}, \frac{6(1 - \rho)}{L_2(s_{\max}^{\text{NC}})^2} \right\}. \quad (9)$$

This unit-step property is characteristic of Newton-type methods (Boyd & Vandenberghe, 2004, Chapter 9). A key consequence of Proposition 3.2 is that our approach introduces a natural scaling to the gradient direction, enabling the backtracking line search to be safely initialized at the unit step size. Moreover, as shown in Theorem 3.6, under certain regularity conditions, the unit step size will satisfy the line search condition (7) for all iterations near a local minimum. In practice, as demonstrated in Section 4, the line search typically accepts  $\alpha = 1$  for most iterations throughout the algorithm’s runtime. This stands in sharp contrast to other first-order algorithms, where the lack of such a mechanism necessitates imposing arbitrary step size ranges.

Once the line search condition (7) is met, the function value decreases by at least  $\rho \alpha \langle \mathbf{p}, \mathbf{g} \rangle = -\rho \alpha \|\mathbf{p}\| \|\mathbf{g}\|$ . Additionally, our analysis in Proposition 3.2 provides a lower bound on the largest step size satisfying (7) at each step. These results ensure global convergence, provided the scaling factor  $s$  in (2) is bounded below. This condition holds automatically for the NC and LPC scalings. For the SPC case, where the scaling is adaptive, we require the following regularity condition on the Hessian.

**Assumption 3.3** (Hessian-gradient Directional Smoothness). There exists  $0 \leq L_1 < \infty$  such that for all  $\mathbf{x} \in \mathbb{R}^d$ , if  $\langle \mathbf{g}(\mathbf{x}), \mathbf{H}(\mathbf{x})\mathbf{g}(\mathbf{x}) \rangle > 0$ , then  $\|\mathbf{H}(\mathbf{x})\mathbf{g}(\mathbf{x})\| \leq L_1 \|\mathbf{g}(\mathbf{x})\|$ .

*Remark 3.4.* For twice continuously differentiable functions, Assumption 3.3 relaxes the standard  $L_{\mathbf{g}}$ -Lipschitz gradient smoothness assumption by requiring regularity only along  $\mathbf{g}$ . Clearly,  $L_1 \leq L_{\mathbf{g}}$ . The concept of *moral smoothness*, introduced in Roosta et al. (2022, Assumption 2), is strictly weaker than Lipschitz gradient and Hessian assumptions on any sublevel set of the gradient norm, yet it still implies Assumption 3.3; see Roosta et al. (2022, Lemma 2).

**Theorem 3.5** (Global Convergence). *Consider Assumptions 3.1 and 3.3 and suppose  $f$  is lower bounded. For any  $0 < \varepsilon_g < 1$ , after at most  $K \in \mathcal{O}(\varepsilon_g^{-2})$  iterations of Algorithm 2, we have  $\|\mathbf{g}_k\| \leq \varepsilon_g$ .*

The detailed complexity bound in Theorem 3.5, including all underlying constants, is provided in Appendix B. Unsurprisingly, the rate in Theorem 3.5 matches that of gradient descent under the Lipschitz gradient smoothness condition with a line search or fixed step size (Cartis et al., 2022; Nesterov, 2004). The novelty of Theorem 3.5 lies in achieving this complexity under the weaker smoothness conditions, i.e., Assumptions 3.1 and 3.3.

#### 3.2. Local Convergence

Let  $\mathbf{x}^*$  be a local minima satisfying the second-order sufficient condition  $\mathbf{g}(\mathbf{x}^*) = 0$  and  $\mathbf{H}(\mathbf{x}^*) \succ 0$ . By the continuity of the Hessian, there exists a ball of radius  $r$  around  $\mathbf{x}^*$ ,

denoted by  $\mathcal{B}_r^*$ , such that

$$0 < \mu \triangleq \min_{\mathbf{x} \in \mathcal{B}_r^*} \lambda_{\min}(\mathbf{H}) \leq \max_{\mathbf{x} \in \mathcal{B}_r^*} \lambda_{\max}(\mathbf{H}) \triangleq M < \infty. \quad (10)$$

Our next result demonstrates that, near  $\mathbf{x}^*$ , the unit step size is acceptable to line search for all iterations, leading to a linear decrease in the sub-optimality of the objective value.

**Theorem 3.6.** *Consider Assumption 3.1 and suppose  $\mathbf{x}^*$  is a local minimum satisfying the second order sufficient conditions. If  $\mathbf{x}_0$  is sufficiently close to  $\mathbf{x}^*$ , then for all iteration of Algorithm 2, the unit step size  $\alpha_k = 1$  satisfies the Armijo condition (7) and we have*

$$f(\mathbf{x}_{k+1}) - f(\mathbf{x}^*) \leq (1 - \tau)(f(\mathbf{x}_k) - f(\mathbf{x}^*)),$$

where  $\tau \triangleq 2\rho\mu \max\{1/M, s_{\min}^{\text{LPC}}\} \in (0, 1]$  if  $\sigma \geq \mu$ , and  $\tau \triangleq 2\rho\mu/M \in (0, 1]$  otherwise.

*Remark 3.7.* Suppose  $\mathbf{x} \in \mathcal{B}_r^*$  where  $\mathcal{B}_r^*$  is as in (10). Since  $\langle \mathbf{g}, \mathbf{H}\mathbf{g} \rangle \leq M \|\mathbf{g}\|^2$ , the SPC case only arises on  $\mathcal{B}_r^*$  if  $\sigma$  is chosen such that  $\sigma \leq M$ ; otherwise Algorithm 1 always returns the LPC scaling. In this case, since  $s_{\min}^{\text{LPC}} < 1/\sigma < 1/M$ , and  $\rho < 1/2$  we always have  $0 < \tau \leq 1$  in Theorem 3.6.

Theorem 3.6 suggests that the rate of convergence for the scaled gradient descent has a similar dependence on the local condition number  $\kappa \triangleq M/\mu$  as that of the typical gradient descent. However, as the proof of Theorem 3.6 reveals, this worst-case analysis overlooks the potential for scaled gradient methods to exploit larger scalings by adapting to local geometry. For instance, if  $\sigma < \mu$  then  $s^{\text{SPC}} \leq 1/\mu$ . Therefore, in “best-case” iterations where large scalings (close to  $1/\mu$ ) pass the line search with unit step size, the linear rate can be as small as  $1 - 2\rho$  (cf. (22)). This rate eliminates dependence on the local condition number, resembling the problem-independent convergence rates of many Newton-type methods (Roosta & Mahoney, 2019; Roosta et al., 2022). In Section 4, we demonstrate numerically that scaled gradient methods often produce large scalings that pass the line search with unit step size, leading to rapid convergence. Conversely, if  $\sigma \gg \mu$ , both LPC and SPC scalings are upper bounded by  $1/\sigma \ll 1/\mu$ , limiting the local rate. These observations suggest that  $\sigma$  should be set relatively small.

Our next result states that the MR scaling (5) can give rise to linear convergence in the gradient norm. Intuitively, this result arises because the MR scaling minimizes the norm of the residual of the Newton system, which can also be viewed as the norm of the linearized gradient.

**Theorem 3.8.** *Consider Assumption 3.1 and suppose  $\mathbf{x}^*$  is a local minimum satisfying the second order sufficient conditions. If  $\mathbf{x}_0$  is sufficiently close to  $\mathbf{x}^*$ , then the iterations of the form  $\mathbf{x}_{k+1} = \mathbf{x}_k - s_k^{\text{MR}} \mathbf{g}_k$  converge linearly in the gradient norm.*

See Appendix B.5 for a proof of this result, which extends beyond second-order sufficient conditions to a more general setting.

An immediate implication of Theorem 3.8 is that the gradient norm serves as a “secondary objective” for the MR scaling. This is notable given recent work on gradient norm regularization, which biases gradient descent toward regions with small gradient norms, often linked to “flat” regions and better generalization in machine learning (Barrett & Dherin, 2021; Smith et al., 2021; Zhao et al., 2022; Karakida et al., 2023; Hochreiter & Schmidhuber, 1997; Keskar et al., 2016). Unlike explicit regularization, which requires additional hyperparameter tuning, MR scaling implicitly achieves this bias without additional considerations.

### 3.3. Inexact Hessian

We now consider the case where the Hessian can only be accessed through an inexact estimate  $\tilde{\mathbf{H}}$ . We show that under certain conditions on the inexactness tolerance, we can attain similar unit step size and convergence guarantees as in the exact case.

**Assumption 3.9** (Hessian Error Bound). For a given  $\Delta_H > 0$  and  $\mathbf{x}$ , we can produce  $\tilde{\mathbf{H}}$  such that

$$\left| \langle \mathbf{g}(\mathbf{x}), (\mathbf{H}(\mathbf{x}) - \tilde{\mathbf{H}}(\mathbf{x}))\mathbf{g}(\mathbf{x}) \rangle \right| \leq \Delta_H \|\mathbf{g}(\mathbf{x})\|^2. \quad (11)$$

This condition requires only that the inexactness is bounded along the gradient direction, a weaker requirement than a direct bound on the difference,  $\mathbf{H}(\mathbf{x}) - \tilde{\mathbf{H}}(\mathbf{x})$ . For a specific case where Assumption 3.9 applies, consider the finite-sum objective where  $f(\mathbf{x}) \triangleq \sum_{i=1}^n f_i(\mathbf{x})/n$ . This formulation arises often in machine learning as part of empirical risk minimization framework (Murphy, 2012). In the “big data” regime, where  $n \gg 1$ , optimization algorithms often use subsampling to estimate gradients or Hessians. Suppose we estimate the Hessian via

$$\tilde{\mathbf{H}}(\mathbf{x}) = \frac{1}{|\mathcal{I}_H|} \sum_{i \in \mathcal{I}_H} \mathbf{H}_i(\mathbf{x}), \quad (12)$$

where  $\mathcal{I}_H \subseteq \{1, \dots, n\}$  is a minibatch of indices uniformly, with replacement. In this case, Assumption 3.9 holds with high probability if the sample size is sufficiently large and the individual Hessians,  $\mathbf{H}_i$ , are uniformly bounded along the gradient direction (see Appendix B.7 for details).

Note that when the estimated Hessian  $\tilde{\mathbf{H}}$  replaces  $\mathbf{H}$  in Algorithm 1, the curvature tests and resulting scalings depend on  $\tilde{\mathbf{H}}$  rather than  $\mathbf{H}$  (see Appendix B.6). Our first result guarantees a unit step size when  $\Delta_H$  is sufficiently small.

**Proposition 3.10.** *Consider Assumption 3.1 and Assumption 3.9 with  $\Delta_H \leq 2 \min\{\sigma(1/2 - \rho), (1 - \rho)/s_{\max}^{\text{NC}}\}$ .*

If

$$\|\mathbf{g}\| \leq 6 \min \left\{ \frac{\sigma^2 \left( \frac{1}{2} - \rho - \frac{\Delta_H}{2\sigma} \right)}{L_2}, \frac{\left( 1 - \rho - \frac{s_{\max}^{NC} \Delta_H}{2} \right)}{L_2 (s_{\max}^{NC})^2} \right\},$$

then the Armijo condition (7) is satisfied with  $\alpha = 1$ .

Using a similar analysis to the exact case, we can also derive a global convergence guarantee for the inexact case, but we require an additional assumption.

**Assumption 3.11** (Inexact Hessian-gradient Smoothness). There exists  $0 \leq \tilde{L}_1 < \infty$  such that for all  $\mathbf{x} \in \mathbb{R}^d$ , we have  $\|\tilde{\mathbf{H}}(\mathbf{x})\mathbf{g}(\mathbf{x})\| \leq \tilde{L}_1 \|\mathbf{g}(\mathbf{x})\|$ .

Much like the exact Hessian case, Assumption 3.11 relaxes the typical Lipschitz gradient assumption used for global convergence in gradient descent. For subsampled Hessians, Assumption 3.11 clearly holds if the individual Hessians,  $\mathbf{H}_i$ , are uniformly bounded along the gradient direction.

The following result shows that, regardless of the Hessian estimation inaccuracy  $\Delta_H$ , the headline convergence rate for the inexact Hessian case matches that of the exact case.

**Proposition 3.12.** Consider Assumption 3.1, Assumption 3.9 for any  $\Delta_H \geq 0$  and Assumption 3.11, and suppose  $f$  is lower bounded. For any  $0 < \varepsilon_g < 1$ , after at most  $K \in \mathcal{O}(\varepsilon_g^{-2})$  iterations of Algorithm 2, with  $\mathbf{H}$  replaced with  $\tilde{\mathbf{H}}$ , we have  $\|\mathbf{g}_k\| \leq \varepsilon_g$ .

Much like Theorem 3.5, the rate obtained in Proposition 3.12 matches the worst case rate for gradient descent on a function with Lipschitz smooth gradients. Interestingly, unlike Proposition 3.10, Proposition 3.12 imposes no specific requirement on  $\Delta_H$ . This is because small step sizes (i.e.,  $\alpha < 1$ ) can mitigate noise when  $\Delta_H$  is large. In Appendix B.6, we discuss how bounding  $\Delta_H$  can improve the per-iteration decrease beyond the worst-case rate for certain steps.

## 4. Numerical Results

We now proceed to validate our results by comparing our scaled gradient method against multiple variants of GD including fixed step size, line search, Nesterov acceleration (Nesterov, 2004), heavy ball momentum (Wright & Recht, 2022), and Adam (Kingma, 2014). We consider each of the CG, MR and GM scalings in our numerical results and, following promising results from Dai & Yuan (2003), in the quadratic case<sup>4</sup>, we also consider various combinations of alternating scalings. The alternating scaling procedure, denoted in our results by a concatenated string of the two

<sup>4</sup>In fact, for two dimensional quadratics, Dai & Yuan (2003) demonstrate that super-linear convergence can be obtained by alternating steepest descent and minimal gradient steps.

scalings, e.g. ‘‘MRCG’’, simply consists of alternating between two scalings, in order, on each SPC iteration<sup>5</sup>. In the main body, we report the best performing scaling, relegating performance comparison between scalings to Appendix D. Where available, we apply theoretically convergent hyperparameter values for our competitor methods, otherwise we manually tune hyperparameter settings. To fairly compare methods with differing per-iteration cost, we plot the objective value against the number of *oracle calls*, i.e., the number of equivalent function evaluations, see Appendix D.1 for details. However, for completeness we also include wall-clock time results in Appendix D. The setup for each problem and optimizer is described in more detail in Appendix D. All methods are implemented in PyTorch (Paszke et al., 2019).

**Multi-class Logistic Regression.** In Figure 1, we present multi-class logistic regression with  $\ell_2$  regularization on the CIFAR10 dataset (Krizhevsky, 2009). This  $\mu$ -strongly convex problem provides a well-behaved, yet challenging, baseline for comparison. We observe that ‘‘MRCG’’ is competitive with Adam and accelerated methods, while significantly outperforming line search and fixed step size approaches. This is achieved without requiring any tuning or prior knowledge of problem constants. Notably, the scalings produced by our method oscillate between large (close to  $1/\mu$ ) and small values throughout the optimization trajectory<sup>6</sup>. Despite the magnitude of these scaling values, the line search accepts the unit step length at *all iterations*, confirming that Proposition 3.2 holds over the entire optimization trajectory. In light of the local convergence property in Theorem 3.6, we believe these large scaling values may contribute to the rapid convergence of our method.

**Multilayer Perceptron (MLP).** In Figure 2, we examine a nonconvex, small MLP on the FashionMNIST dataset (Xiao et al., 2017). The results show that ‘‘CGMR’’ scaled gradient is again competitive with Adam and significantly outperforms all other methods, all without requiring hyperparameter tuning. Notably, similar to the logistic regression experiment, the unit step size is accepted by the line search at every iteration, except for one where NC is detected and exploited using forward tracking search. Meanwhile, LPC does not occur at any point during the optimization trajectory. The scaling chosen by CGMR oscillates between large and small values, mirroring the behavior observed in the convex logistic regression experiment.

**Resnet.** In Figure 3, we examine an over-parameterized, nonconvex ResNet18 architecture (He et al., 2016) on the Imagenette dataset (Howard, 2019). For this experiment, we run our scaling methods with a fixed unit step size instead of

<sup>5</sup>If an LPC/NC arises, we proceed based on the last SPC step.

<sup>6</sup>As shown in Appendix D.2, this ‘‘large scaling’’ effect is most pronounced for alternating scaling.

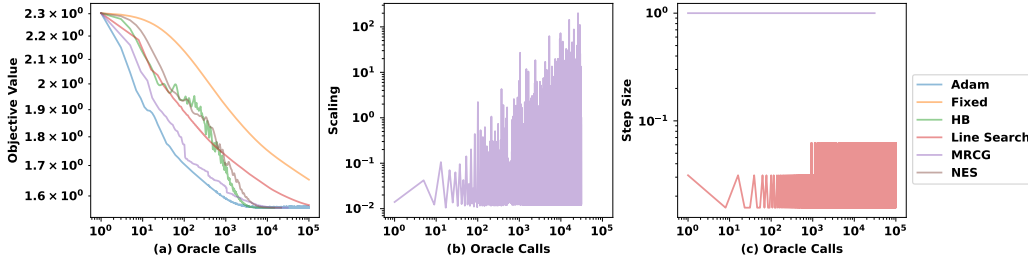


Figure 1. Multi-class logistic regression on CIFAR10. (a) The objective value. (b) The scaling utilized by the MRCG method. (c) The step size selected by line search, for applicable methods.

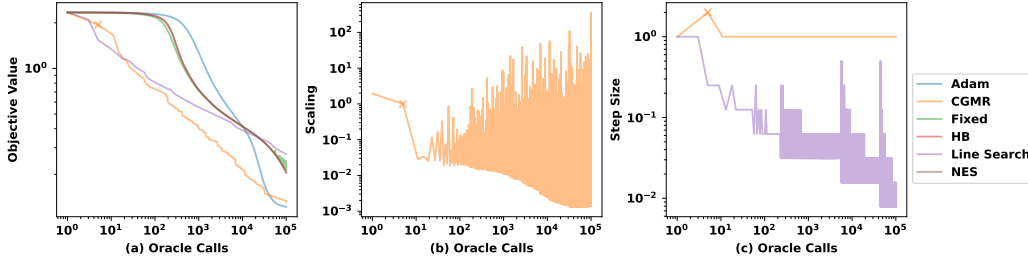


Figure 2. MLP on the FashionMNIST. (a) The objective value (b) The scaling utilized by the CGMR method (c) The step size selected by line search, for applicable methods. Crosses indicate iterations where negative curvature is detected.

line search. The results show that the scaled gradient method MRCG reduces the function value monotonically throughout the optimization trajectory, with no NC or LPC directions detected during the iterations. Our method significantly outperforms the only other adaptive method (line search) but is surpassed by hyperparameter-tuned approaches. In contrast to scaled gradient, the tuned methods exhibit notable instability in the early iterations, followed by stabilization and convergence. This “unstable convergence” effect has been observed to be beneficial in many large-scale, nonconvex models (Cohen et al., 2021; Ahn et al., 2022). Given this, it appears that for scaled gradient to be competitive on large-scale problems, some degree of non-monotonicity must be introduced into the iterations. Fortunately, Roulet et al. (2024) demonstrate that by using CG-style scaling with large step sizes (e.g.,  $\alpha \geq 2$ ), unstable convergence can be induced in a principled<sup>7</sup> manner. A similar approach could be applied to our methods to design *principled* step size schedules, such as annealing from  $\alpha \geq 2$  (unstable) to  $\alpha = 1$  (stable), to leverage the benefits of the unstable regime. We leave this exploration for future work.

Finally, we note that the MR scaling uniformly decreases the gradient with the unit step size across our examples, consistent with Theorem 3.8; see Appendix D.

<sup>7</sup>Specifically, a step size of  $\alpha = 2$  with CG scaling implies *non-decrease* in the local quadratic model along the search direction.

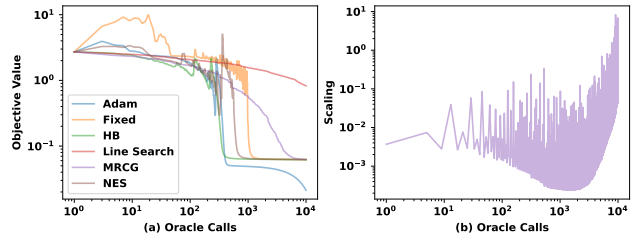


Figure 3. ResNet18 on Imagenette. (a) The objective value. (b) The scaling utilized by the MRCG method.

## 5. Conclusions and Future Directions

We developed a framework based on (weakened) Lipschitz Hessian smoothness for analyzing Hessian-aware scaling of gradient directions. Under this framework, we show that Hessian curvature information can be used to enhance vanilla GD with a unit step size guarantee. We show this guarantee holds for all iterations near minima satisfying certain regularity conditions. Furthermore, with a weakened Lipschitz gradient smoothness, we prove global convergence. Numerically, we observe that the unit step size guarantee holds across most of the optimization trajectory. We also demonstrate that alternating scalings can achieve fast monotonic convergence on medium-scale problems.

A limitation of our results is the performance on large-scale nonconvex models. However, principled step size sched-



ules, scaling for momentum and adaptive gradient methods, and stochastic gradient variations can be viewed as natural extensions of our analysis, offering potential avenues for future research to address this limitation.

## Acknowledgments

Roosta was partially supported by the Australian Research Council through an Industrial Transformation Training Centre for Information Resilience (IC200100022). Wright was partially supported by the US National Science Foundation under grants CCF 2224213 and DMS 2023239.

## References

- Ahn, K., Zhang, J., and Sra, S. Understanding the unstable convergence of gradient descent. In Chaudhuri, K., Jegelka, S., Song, L., Szepesvari, C., Niu, G., and Sabato, S. (eds.), *Proceedings of the 39th International Conference on Machine Learning*, volume 162 of *Proceedings of Machine Learning Research*, pp. 247–257. PMLR, 17–23 Jul 2022. URL <https://proceedings.mlr.press/v162/ahn22a.html>.
- Altschuler, J. and Parrilo, P. Acceleration by stepsize hedging: Multi-step descent and the silver stepsize schedule. *J. ACM*, December 2024. ISSN 0004-5411. doi: 10.1145/3708502. URL <https://doi.org/10.1145/3708502>.
- Ba, J. L., Kiros, J. R., and Hinton, G. E. Layer normalization, 2016. URL <https://arxiv.org/abs/1607.06450>.
- Barrett, D. and Dherin, B. Implicit gradient regularization. In *International Conference on Learning Representations*, 2021. URL <https://openreview.net/forum?id=3q5IqUrkcF>.
- Barzilai, J. and Borwein, J. M. Two-point step size gradient methods. *IMA Journal of Numerical Analysis*, 8(1):141–148, 01 1988. ISSN 0272-4979. URL <https://doi.org/10.1093/imanum/8.1.141>.
- Baydin, A. G., Pearlmutter, B. A., Radul, A. A., and Siskind, J. M. Automatic differentiation in machine learning: A survey. *Journal of Machine Learning Research*, 18(153): 1–43, 2018.
- Berahas, A. S., Roberts, L., and Roosta, F. Non-uniform smoothness for gradient descent. *Transactions on Machine Learning Research*, 2024. ISSN 2835-8856.
- Blondel, M. and Roulet, V. The elements of differentiable programming, 2024. URL <https://arxiv.org/abs/2403.14606>.
- Boyd, S. P. and Vandenberghe, L. *Convex Optimization*. Cambridge University Press, Cambridge, UK ; New York, 2004. ISBN 978-0-521-83378-3.
- Cartis, C., Gould, N. I. M., and Toint, P. L. *Evaluation Complexity of Algorithms for Nonconvex Optimization: Theory, Computation, and Perspectives*. Society for Industrial and Applied Mathematics, Philadelphia, 2022. ISBN 978-1-61197-699-1.
- Castera, C., Bolte, J., Févotte, C., and Pauwels, E. Second-Order Step-Size Tuning of SGD for Non-Convex Optimization. *Neural Processing Letters*, 54(3):1727–1752, June 2022. ISSN 1370-4621, 1573-773X. doi: 10.1007/s11063-021-10705-5.
- Cohen, J., Kaur, S., Li, Y., Kolter, J. Z., and Talwalkar, A. Gradient descent on neural networks typically occurs at the edge of stability. In *International Conference on Learning Representations*, 2021. URL <https://openreview.net/forum?id=jh-rTtvkGeM>.
- Curtis, F. E. and Robinson, D. P. Exploiting negative curvature in deterministic and stochastic optimization. *Mathematical Programming*, 176(1-2):69–94, July 2019. ISSN 0025-5610, 1436-4646. doi: 10.1007/s10107-018-1335-8.
- Dai, Y. H. and Yang, X. Q. A New Gradient Method with an Optimal Step-size Property. *Computational Optimization and Applications*, 33(1):73–88, January 2006. ISSN 0926-6003, 1573-2894. doi: 10.1007/s10589-005-5959-2.
- Dai, Y.-H. and Yuan, Y.-X. Alternate minimization gradient method. *IMA Journal of Numerical Analysis*, 23:377–393, 2003.
- Dai, Y.-H., Huang, Y., and Liu, X.-W. A family of spectral gradient methods for optimization. *Computational Optimization and Applications*, 74(1):43–65, September 2019. ISSN 0926-6003, 1573-2894. doi: 10.1007/s10589-019-00107-8.
- de Gournay, F. and Gossard, A. Adaptive scaling of the learning rate by second order automatic differentiation. *arXiv preprint arXiv:2210.14520*, 2022.
- Defazio, A. and Mishchenko, K. Learning-rate-free learning by D-adaptation. In Krause, A., Brunskill, E., Cho, K., Engelhardt, B., Sabato, S., and Scarlett, J. (eds.), *Proceedings of the 40th International Conference on Machine Learning*, volume 202 of *Proceedings of Machine Learning Research*, pp. 7449–7479. PMLR, 23–29 Jul 2023. URL <https://proceedings.mlr.press/v202/defazio23a.html>.

- Deng, J., Dong, W., Socher, R., Li, L.-J., Li, K., and Fei-Fei, L. Imagenet: A large-scale hierarchical image database. In *2009 IEEE conference on computer vision and pattern recognition*, pp. 248–255. Ieee, 2009.
- Drineas, P., Kannan, R., and Mahoney, M. W. Fast Monte Carlo algorithms for matrices I: Approximating matrix multiplication. *SIAM Journal on Computing*, 36(1):132–157, 2006. doi: 10.1137/S0097539704442684. URL <https://doi.org/10.1137/S0097539704442684>.
- Fletcher, R. On the Barzilai-Borwein Method. In Qi, L., Teo, K., and Yang, X. (eds.), *Optimization and Control with Applications*, volume 96, pp. 235–256. Springer-Verlag, New York, 2005. ISBN 978-0-387-24254-5. doi: 10.1007/0-387-24255-4\_10.
- Gonzaga, C. C. and Schneider, R. M. On the steepest descent algorithm for quadratic functions. *Computational Optimization and Applications*, 63(2):523–542, March 2016. ISSN 0926-6003, 1573-2894. doi: 10.1007/s10589-015-9775-z.
- Goodfellow, I., Bengio, Y., and Courville, A. *Deep Learning*. MIT press, 2016.
- Gould, N. I. M., Lucidi, S., Roma, M., and Toint, Ph. L. Exploiting negative curvature directions in linesearch methods for unconstrained optimization. *Optimization Methods and Software*, 14(1-2):75–98, January 2000. ISSN 1055-6788, 1029-4937. doi: 10.1080/10556780008805794.
- Grimmer, B. Provably faster gradient descent via long steps. *SIAM Journal on Optimization*, 34(3):2588–2608, 2024. doi: 10.1137/23M1588408. URL <https://doi.org/10.1137/23M1588408>.
- He, K., Zhang, X., Ren, S., and Sun, J. Deep residual learning for image recognition. In *2016 IEEE Conference on Computer Vision and Pattern Recognition (CVPR)*, pp. 770–778, 2016. doi: 10.1109/CVPR.2016.90.
- Hendrycks, D. and Gimpel, K. Gaussian error linear units (gelus). *arXiv preprint arXiv:1606.08415*, 2016.
- Hochreiter, S. and Schmidhuber, J. Flat Minima. *Neural Computation*, 9(1):1–42, 01 1997. ISSN 0899-7667. doi: 10.1162/neco.1997.9.1.1. URL <https://doi.org/10.1162/neco.1997.9.1.1>.
- Howard, J. Imagenette: A smaller subset of 10 easily classified classes from Imagenet, March 2019. URL <https://github.com/fastai/imagenette>.
- Ioffe, S. and Szegedy, C. Batch normalization: accelerating deep network training by reducing internal covariate shift. In *Proceedings of the 32nd International Conference on International Conference on Machine Learning - Volume 37*, ICML’15, pp. 448–456. JMLR.org, 2015.
- Ivgi, M., Hinder, O., and Carmon, Y. DoG is SGD’s best friend: A parameter-free dynamic step size schedule. In *International Conference on Machine Learning*, pp. 14465–14499. PMLR, 2023.
- Karakida, R., Takase, T., Hayase, T., and Osawa, K. Understanding gradient regularization in deep learning: Efficient finite-difference computation and implicit bias. In *International Conference on Machine Learning*, pp. 15809–15827. PMLR, 2023.
- Keskar, N. S., Mudigere, D., Nocedal, J., Smelyanskiy, M., and Tang, P. T. P. On large-batch training for deep learning: Generalization gap and sharp minima. *arXiv preprint arXiv:1609.04836*, 2016.
- Khaled, A., Mishchenko, K., and Jin, C. DoWG unleashed: An efficient universal parameter-free gradient descent method. *Advances in Neural Information Processing Systems*, 36:6748–6769, 2023.
- Kingma, D. P. Adam: A method for stochastic optimization. *arXiv preprint arXiv:1412.6980*, 2014.
- Krizhevsky, A. Learning multiple layers of features from tiny images. Technical report, University of Toronto, 2009.
- Lan, G. *First-Order and Stochastic Optimization Methods for Machine Learning*. Springer Series in the Data Sciences. Springer International Publishing, Cham, 2020. ISBN 978-3-030-39567-4 978-3-030-39568-1. doi: 10.1007/978-3-030-39568-1.
- Lim, A. and Roosta, F. Complexity guarantees for non-convex Newton-MR under inexact Hessian information. *arXiv preprint arXiv:2308.09912*, 2023.
- Liu, Y. and Roosta, F. A Newton-MR algorithm with complexity guarantees for nonconvex smooth unconstrained optimization. *arXiv preprint arXiv:2208.07095*, 2022.
- Loizou, N., Vaswani, S., Laradji, I., and Lacoste-Julien, S. Stochastic Polyak Step-size for SGD: An Adaptive Learning Rate for Fast Convergence. In *24th International Conference on Artificial Intelligence and Statistics*, 2021.
- MacDonald, L., Murray, R., and Tappenden, R. On a family of relaxed gradient descent methods for quadratic minimization. *arXiv preprint arXiv:2404.19255*, 2024.
- Malitsky, Y. and Mishchenko, K. Adaptive gradient descent without descent. In III, H. D. and Singh, A. (eds.), *Proceedings of the 37th International Conference on Machine Learning*, volume 119 of *Proceedings of Machine*

- Learning Research*, pp. 6702–6712. PMLR, 13–18 Jul 2020. URL <https://proceedings.mlr.press/v119/malitsky20a.html>.
- Malitsky, Y. and Mishchenko, K. Adaptive proximal gradient method for convex optimization. In *The Thirty-eighth Annual Conference on Neural Information Processing Systems*, 2024. URL <https://openreview.net/forum?id=qlH21Igl1IC>.
- Martens, J. Deep learning via Hessian-free optimization. In *Proceedings of the 27th International Conference on International Conference on Machine Learning*, pp. 735–742, 2010.
- Martens, J. and Grosse, R. Optimizing neural networks with Kronecker-factored approximate curvature. In *International conference on machine learning*, pp. 2408–2417. PMLR, 2015.
- Mishchenko, K. and Defazio, A. Prodigy: an expeditiously adaptive parameter-free learner. In *Proceedings of the 41st International Conference on Machine Learning, ICML’24*. JMLR.org, 2024.
- Mishkin, A., Khaled, A., Wang, Y., Defazio, A., and Gower, R. M. Directional smoothness and gradient methods: Convergence and adaptivity. *arXiv preprint arXiv:2403.04081*, 2024.
- Murphy, K. P. *Machine Learning: A Probabilistic Perspective*. Adaptive Computation and Machine Learning Series. MIT Press, Cambridge, MA, 2012. ISBN 978-0-262-01802-9.
- Nesterov, Y. *Introductory Lectures on Convex Optimization*, volume 87 of *Applied Optimization*. Springer US, Boston, MA, 2004. ISBN 978-1-4613-4691-3 978-1-4419-8853-9. doi: 10.1007/978-1-4419-8853-9.
- Nesterov, Y. and Polyak, B. Cubic regularization of Newton method and its global performance. *Mathematical Programming*, 108(1):177–205, August 2006. ISSN 0025-5610, 1436-4646. doi: 10.1007/s10107-006-0706-8.
- Nocedal, J. and Wright, S. J. *Numerical Optimization*. Springer Series in Operation Research and Financial Engineering. Springer, New York, NY, second edition edition, 2006. ISBN 978-0-387-30303-1 978-1-4939-3711-0.
- Oikonomou, D. and Loizou, N. Stochastic Polyak step-sizes and momentum: Convergence guarantees and practical performance. *arXiv preprint arXiv:2406.04142*, 2024.
- Orvieto, A., Lacoste-Julien, S., and Loizou, N. Dynamics of SGD with stochastic Polyak stepsizes: Truly adaptive variants and convergence to exact solution. *Advances in Neural Information Processing Systems*, 35:26943–26954, 2022.
- Paige, C. C. and Saunders, M. A. Solution of sparse indefinite systems of linear equations. *SIAM Journal on Numerical Analysis*, 12(4):617–629, 1975. doi: 10.1137/0712047. URL <https://doi.org/10.1137/0712047>.
- Paszke, A., Gross, S., Massa, F., Lerer, A., Bradbury, J., Chanan, G., Killeen, T., Lin, Z., Gimelshein, N., Antiga, L., Desmaison, A., Kopf, A., Yang, E., DeVito, Z., Raison, M., Tejani, A., Chilamkurthy, S., Steiner, B., Fang, L., Bai, J., and Chintala, S. PyTorch: An imperative style, high-performance deep learning library. In Wallach, H., Larochelle, H., Beygelzimer, A., d’Alché-Buc, F., Fox, E., and Garnett, R. (eds.), *Advances in Neural Information Processing Systems*, volume 32. Curran Associates, Inc., 2019. URL [https://proceedings.neurips.cc/paper\\_files/paper/2019/file/bdbca288fee7f92f2bfa9f7012727740-Paper.pdf](https://proceedings.neurips.cc/paper_files/paper/2019/file/bdbca288fee7f92f2bfa9f7012727740-Paper.pdf).
- Patel, V. and Berahas, A. S. Gradient descent in the absence of global Lipschitz continuity of the gradients. *SIAM Journal on Mathematics of Data Science*, 6(3):602–626, 2024.
- Patel, V., Zhang, S., and Tian, B. Global convergence and stability of stochastic gradient descent. *Advances in Neural Information Processing Systems*, 35:36014–36025, 2022.
- Pearlmutter, B. A. Fast Exact Multiplication by the Hessian. *Neural Computation*, 6(1):147–160, jan 1994. ISSN 0899-7667, 1530-888X. doi: 10.1162/neco.1994.6.1.147.
- Polyak, B. T. *Introduction to Optimization*. Translations series in mathematics and engineering. Optimization Software, Publications Division, New York, 1987. ISBN 978-0-911575-14-9.
- Roosta, F. and Mahoney, M. W. Sub-sampled Newton methods. *Mathematical Programming*, 174(1-2):293–326, March 2019. ISSN 0025-5610, 1436-4646. doi: 10.1007/s10107-018-1346-5.
- Roosta, F., Liu, Y., Xu, P., and Mahoney, M. W. NewtonMR: Inexact Newton Method with minimum residual sub-problem solver. *EURO Journal on Computational Optimization*, 10:100035, 2022. ISSN 21924406. doi: 10.1016/j.ejco.2022.100035.
- Roulet, V., Agarwala, A., Grill, J.-B., Swirszcz, G. M., Blondel, M., and Pedregosa, F. Stepping on the edge: Curvature aware learning rate tuners. In *The Thirty-eighth Annual Conference on Neural Information Processing Systems*, 2024.

- Smee, O. and Roosta, F. Inexact Newton-type Methods for Optimisation with Nonnegativity Constraints. In *Forty-First International Conference on Machine Learning*, 2024.
- Smith, S. L., Dherin, B., Barrett, D., and De, S. On the origin of implicit regularization in stochastic gradient descent. In *International Conference on Learning Representations*, 2021.
- Wright, S. J. and Recht, B. *Optimization for Data Analysis*. Cambridge University Press, 1 edition, March 2022. ISBN 978-1-00-900428-2 978-1-316-51898-4. doi: 10.1017/9781009004282.
- Wu, Y. and He, K. Group normalization. In *Proceedings of the European Conference on Computer Vision (ECCV)*, September 2018.
- Xiao, H., Rasul, K., and Vollgraf, R. Fashion-MNIST: a novel image dataset for benchmarking machine learning algorithms. *arXiv preprint arXiv:1708.07747*, 2017.
- Zhao, Y., Zhang, H., and Hu, X. Penalizing Gradient Norm for Efficiently Improving Generalization in Deep Learning. In *International Conference on Machine Learning*. PMLP, 2022.

## A. Additional Material for Section 2

### Proof of Proposition 2.2

*Proof.* In the  $\text{LPC}$  and  $\text{NC}$  cases, the results follow from the definition of  $s^{\text{LPC}}$  and  $s^{\text{NC}}$  in Algorithm 1. The  $\text{SPC}$  condition excludes the case where  $\mathbf{g} = 0$ , furthermore, it is clear that  $\langle \mathbf{g}, \mathbf{H}\mathbf{g} \rangle > 0$  implies  $\mathbf{H}\mathbf{g} \neq 0$ , and hence all of the scalings are well defined. The Cauchy-Schwarz inequality implies  $\langle \mathbf{g}, \mathbf{H}\mathbf{g} \rangle \leq \|\mathbf{g}\| \|\mathbf{H}\mathbf{g}\|$  and  $\|\mathbf{H}\mathbf{g}\| \geq \langle \mathbf{g}, \mathbf{H}\mathbf{g} \rangle / \|\mathbf{g}\|$ . Applying these two inequalities subsequently to  $s^{\text{MR}}$  we have

$$0 < s^{\text{MR}} = \frac{\langle \mathbf{g}, \mathbf{H}\mathbf{g} \rangle}{\|\mathbf{H}\mathbf{g}\|^2} \leq \frac{\|\mathbf{g}\|}{\|\mathbf{H}\mathbf{g}\|} \leq \frac{\|\mathbf{g}\|^2}{\langle \mathbf{g}, \mathbf{H}\mathbf{g} \rangle},$$

which captures the three left inequalities in this case. The right-most inequality follows from  $\langle \mathbf{g}, \mathbf{H}\mathbf{g} \rangle > \sigma \|\mathbf{g}\|^2$  and the definition of (4).  $\square$

### Proof of Proposition 2.3

*Proof.* The first-order descent trivially holds. In the  $\text{NC}$  case, the result immediately follows from  $\langle \mathbf{p}, \mathbf{H}\mathbf{p} \rangle < 0$  and the first-order descent property. In the  $\text{LPC}$  case,

$$\begin{aligned} \langle \mathbf{g}, \mathbf{p} \rangle + \langle \mathbf{p}, \mathbf{H}\mathbf{p} \rangle &= -s^{\text{LPC}} \|\mathbf{g}\|^2 + (s^{\text{LPC}})^2 \langle \mathbf{g}, \mathbf{H}\mathbf{g} \rangle \\ &\leq -s^{\text{LPC}} \|\mathbf{g}\|^2 + (s^{\text{LPC}})^2 \sigma \|\mathbf{g}\|^2 \\ &\leq -s^{\text{LPC}} \|\mathbf{g}\|^2 + s^{\text{LPC}} \|\mathbf{g}\|^2 = 0, \end{aligned}$$

where the second to last line follows from the  $\text{LPC}$  condition and the last line follows from  $s^{\text{LPC}} \leq 1/\sigma$  in Proposition 2.2.

For the  $\text{SPC}$  case, we consider each scaling successively. For the  $\text{CG}$  scaling, we have

$$\begin{aligned} \langle \mathbf{p}^{\text{CG}}, \mathbf{g} \rangle + \langle \mathbf{p}^{\text{CG}}, \mathbf{H}\mathbf{p}^{\text{CG}} \rangle &= -s^{\text{CG}} \|\mathbf{g}\|^2 + (s^{\text{CG}})^2 \langle \mathbf{g}, \mathbf{H}\mathbf{g} \rangle \\ &= -\frac{\|\mathbf{g}\|^4}{\langle \mathbf{g}, \mathbf{H}\mathbf{g} \rangle} + \frac{\|\mathbf{g}\|^4}{(\langle \mathbf{g}, \mathbf{H}\mathbf{g} \rangle)^2} \langle \mathbf{g}, \mathbf{H}\mathbf{g} \rangle \\ &= 0. \end{aligned}$$

For the  $\text{MR}$  scaling, we have

$$\begin{aligned} \langle \mathbf{p}^{\text{MR}}, \mathbf{g} \rangle + \langle \mathbf{p}^{\text{MR}}, \mathbf{H}\mathbf{p}^{\text{MR}} \rangle &= -s^{\text{MR}} \|\mathbf{g}\|^2 + (s^{\text{MR}})^2 \langle \mathbf{g}, \mathbf{H}\mathbf{g} \rangle \\ &= -\frac{\langle \mathbf{g}, \mathbf{H}\mathbf{g} \rangle}{\|\mathbf{H}\mathbf{g}\|^2} \|\mathbf{g}\|^2 + \frac{(\langle \mathbf{g}, \mathbf{H}\mathbf{g} \rangle)^2}{\|\mathbf{H}\mathbf{g}\|^4} \langle \mathbf{g}, \mathbf{H}\mathbf{g} \rangle \\ &\leq -\frac{\langle \mathbf{g}, \mathbf{H}\mathbf{g} \rangle}{\|\mathbf{H}\mathbf{g}\|^2} \|\mathbf{g}\|^2 + \frac{\|\mathbf{g}\|^2}{\|\mathbf{H}\mathbf{g}\|^2} \langle \mathbf{g}, \mathbf{H}\mathbf{g} \rangle \\ &= 0, \end{aligned}$$

where the third line follows from the Cauchy-Schwarz inequality. Finally, for the geometric mean scaling, we have

$$\begin{aligned} \langle \mathbf{p}^{\text{GM}}, \mathbf{g} \rangle + \langle \mathbf{p}^{\text{GM}}, \mathbf{H}\mathbf{p}^{\text{GM}} \rangle &= -s^{\text{GM}} \|\mathbf{g}\|^2 + (s^{\text{GM}})^2 \langle \mathbf{g}, \mathbf{H}\mathbf{g} \rangle \\ &= -\frac{\|\mathbf{g}\|^3}{\|\mathbf{H}\mathbf{g}\|} + \frac{\|\mathbf{g}\|^2}{\|\mathbf{H}\mathbf{g}\|^2} \langle \mathbf{g}, \mathbf{H}\mathbf{g} \rangle \\ &\leq -\frac{\|\mathbf{g}\|^3}{\|\mathbf{H}\mathbf{g}\|} + \frac{\|\mathbf{g}\|^2}{\|\mathbf{H}\mathbf{g}\|^2} \|\mathbf{g}\| \|\mathbf{H}\mathbf{g}\| \\ &= -\frac{\|\mathbf{g}\|^3}{\|\mathbf{H}\mathbf{g}\|} + \frac{\|\mathbf{g}\|^3}{\|\mathbf{H}\mathbf{g}\|} = 0, \end{aligned}$$

where again the third line follows from the Cauchy-Schwarz inequality.  $\square$

### Proof of Proposition 2.5

*Proof.* Consider a scalar reparameterization of the original variables  $\mathbf{x}$  as  $\mathbf{y} = \mathbf{x}/c$ , for some  $c \neq 0$ . Our objective over the new coordinates is  $\bar{f}(\mathbf{y}) = f(c\mathbf{y})$  so that

$$\nabla_{\mathbf{y}} \bar{f}(\mathbf{y}) = c \nabla f(\mathbf{x}), \quad \nabla_{\mathbf{y}}^2 \bar{f}(\mathbf{y}) = c^2 \nabla^2 f(\mathbf{x}).$$

Therefore, SPC scalings computed in the transformed coordinates satisfy

$$s(\mathbf{y}) = \frac{s(\mathbf{x})}{c^2}.$$

For example, for the MR scaling we have

$$s^{\text{MR}}(\mathbf{y}) = \frac{\langle \nabla_{\mathbf{y}} \bar{f}(\mathbf{y}), \nabla_{\mathbf{y}}^2 \bar{f}(\mathbf{y}) \nabla_{\mathbf{y}} \bar{f}(\mathbf{y}) \rangle}{\|\nabla_{\mathbf{y}}^2 \bar{f}(\mathbf{y}) \nabla_{\mathbf{y}} \bar{f}(\mathbf{y})\|^2} = \frac{\langle c \nabla f(\mathbf{x}), (c^2 \nabla^2 f(\mathbf{x})) c \nabla f(\mathbf{x}) \rangle}{\|c^2 \nabla^2 f(\mathbf{x}) c \nabla f(\mathbf{x})\|^2} = \frac{1}{c^2} s^{\text{MR}}(\mathbf{x}).$$

Now this implies that, for the SPC scaled gradient directions, the update computed with respect to the new coordinates preserves the reparameterization. Indeed, given  $\mathbf{y}_k = \mathbf{x}_k/c$ , the scaled gradient descent update at  $\mathbf{y}_k$  with some fixed step size  $\alpha > 0$  is

$$\mathbf{y}_{k+1} = \mathbf{y}_k - \alpha s(\mathbf{y}_k) \nabla_{\mathbf{y}} \bar{f}(\mathbf{y}_k) = \frac{1}{c} (\mathbf{x}_k - \alpha s(\mathbf{x}_k) \nabla f(\mathbf{x}_k)) = \frac{\mathbf{x}_{k+1}}{c},$$

where  $\mathbf{x}_{k+1} = \mathbf{x}_k - \alpha s(\mathbf{x}_k) \nabla f(\mathbf{x}_k)$  is the update in the original coordinates. That is, the same relationship between  $\mathbf{x}$  and  $\mathbf{y}$  holds at the following iteration.  $\square$

## B. Additional Material for Section 3

### B.1. Line Search Algorithms

---

**Algorithm 3** Backward Tracking Line Search.

---

- 1: **input:** Initial step size  $\alpha_0 = 1$ , Scaling parameter  $0 < \theta < 1$ .
  - 2:  $\alpha \leftarrow \alpha_0$ .
  - 3: **while** (7) is not satisfied **do**
  - 4:    $\alpha \leftarrow \theta \alpha$ .
  - 5: **end while**
  - 6: **return**  $\alpha$ .
- 

---

**Algorithm 4** Forward/Backward Tracking Line Search

---

- 1: **input:** Initial step size  $\alpha_0 = 1$ , Scaling parameter  $0 < \theta < 1$ .
  - 2:  $\alpha \leftarrow \alpha_0$ .
  - 3: **if** (7) is not satisfied **then**
  - 4:   Call Algorithm 3
  - 5: **else**
  - 6:   **while** (7) is satisfied **do**
  - 7:      $\alpha = \alpha/\theta$ .
  - 8:   **end while**
  - 9:   **return**  $\theta \alpha$ .
  - 10: **end if**
-

## B.2. Derivation and Proof of Proposition 3.2

Throughout the following we routinely make use of the facts, due to collinearity of  $\mathbf{g}$  and  $\mathbf{p}$ , that  $\langle \mathbf{p}, \mathbf{g} \rangle = -\|\mathbf{p}\| \|\mathbf{g}\|$ ,  $\|\mathbf{p}\| = s \|\mathbf{g}\|$ , and the fact that  $\langle \mathbf{g}, \mathbf{H}\mathbf{g} \rangle$  and  $\langle \mathbf{p}, \mathbf{H}\mathbf{p} \rangle$  have the same sign. Also, letting  $\mathbf{p} = -s\mathbf{g}$ ,  $s \geq 0$ , Assumption 3.1 and twice continuous differentiability of  $f$  imply

$$\|\mathbf{g}(\mathbf{x} + \mathbf{p}) - \mathbf{g}(\mathbf{x}) - \mathbf{H}(\mathbf{x})\mathbf{p}\| \leq \frac{L_2}{2} \|\mathbf{p}\|^2, \quad (13)$$

$$\left| f(\mathbf{x} + \mathbf{p}) - f(\mathbf{x}) - \langle \mathbf{g}, \mathbf{p} \rangle - \frac{1}{2} \langle \mathbf{p}, \mathbf{H}\mathbf{p} \rangle \right| \leq \frac{L_2}{6} \|\mathbf{p}\|^3. \quad (14)$$

These bounds can be derived similarly to the general Lipschitz Hessian upper bounds in, e.g., [Nesterov & Polyak \(2006, Lemma 1\)](#). Our analysis is based on applying the second order descent condition (3) to the cubic upper bound in (14). We consider the non-negative and negative curvature cases separately.

**Non-negative Curvature Case.** Suppose the curvature along the gradient direction is nonnegative, i.e.,  $\langle \mathbf{g}, \mathbf{H}\mathbf{g} \rangle \geq 0$ . In this case, Algorithm 1 selects either the SPC or LPC scalings. By Propositions 2.2 and 2.3, we have  $s \leq 1/\sigma$  and (3). Considering (14) and applying  $\alpha \leq 1$  and (3), we have

$$\begin{aligned} f(\mathbf{x} + \alpha\mathbf{p}) &\leq f(\mathbf{x}) + \alpha \langle \mathbf{g}, \mathbf{p} \rangle + \frac{\alpha^2}{2} \langle \mathbf{p}, \mathbf{H}\mathbf{p} \rangle + \frac{L_2\alpha^3}{6} \|\mathbf{p}\|^3 \\ &\leq f(\mathbf{x}) + \frac{\alpha}{2} \langle \mathbf{g}, \mathbf{p} \rangle + \frac{\alpha}{2} (\langle \mathbf{g}, \mathbf{p} \rangle + \langle \mathbf{p}, \mathbf{H}\mathbf{p} \rangle) + \frac{L_2\alpha^3}{6} \|\mathbf{p}\|^3 \\ &\leq f(\mathbf{x}) + \frac{\alpha}{2} \langle \mathbf{g}, \mathbf{p} \rangle + \frac{L_2\alpha^3}{6} \|\mathbf{p}\|^3. \end{aligned}$$

Subtracting  $f(\mathbf{x}) + \alpha\rho \langle \mathbf{p}, \mathbf{g} \rangle$  from both sides yields

$$\begin{aligned} f(\mathbf{x} + \alpha\mathbf{p}) - f(\mathbf{x}) - \alpha\rho \langle \mathbf{p}, \mathbf{g} \rangle &\leq \alpha \left( \frac{1}{2} - \rho \right) \langle \mathbf{p}, \mathbf{g} \rangle + \frac{L_2\alpha^3}{6} \|\mathbf{p}\|^3 \\ &= -\alpha \left( \frac{1}{2} - \rho \right) \|\mathbf{g}\| \|\mathbf{p}\| + \frac{L_2\alpha^3}{6} s \|\mathbf{g}\| \|\mathbf{p}\|^2 \\ &= \left( \rho - \frac{1}{2} + \frac{L_2\alpha^2 s \|\mathbf{p}\|}{6} \right) \alpha \|\mathbf{p}\| \|\mathbf{g}\| \\ &\leq \left( \rho - \frac{1}{2} + \frac{L_2\alpha^2 \|\mathbf{p}\|}{6\sigma} \right) \alpha \|\mathbf{p}\| \|\mathbf{g}\|, \end{aligned}$$

where the last inequality follows from  $s \leq 1/\sigma$ . This implies (7) holds if

$$\alpha \leq \min \left\{ 1, \sqrt{\frac{6\sigma(1/2 - \rho)}{L_2 \|\mathbf{p}\|}} \right\}. \quad (15)$$

**Negative Curvature Case.** We now consider the case where  $\langle \mathbf{g}, \mathbf{H}\mathbf{g} \rangle < 0$ , in which case Algorithm 1 selects the NC scaling. As a result, dropping the negative term in (14) gives

$$\begin{aligned} f(\mathbf{x} + \alpha\mathbf{p}) &\leq f(\mathbf{x}) + \alpha \langle \mathbf{p}, \mathbf{g} \rangle + \frac{\alpha^2}{2} \langle \mathbf{p}, \mathbf{H}\mathbf{p} \rangle + \frac{L_2\alpha^3}{6} \|\mathbf{p}\|^3 \\ &\leq f(\mathbf{x}) + \alpha \langle \mathbf{p}, \mathbf{g} \rangle + \frac{L_2\alpha^3}{6} \|\mathbf{p}\|^3. \end{aligned}$$

Similarly to the previous case, subtracting  $f(\mathbf{x}) + \alpha\rho \langle \mathbf{p}, \mathbf{g} \rangle$  yields

$$\begin{aligned} f(\mathbf{x} + \alpha\mathbf{p}) - f(\mathbf{x}) - \alpha\rho \langle \mathbf{p}, \mathbf{g} \rangle &\leq \alpha(1 - \rho) \langle \mathbf{p}, \mathbf{g} \rangle + \frac{L_2\alpha^3}{6} \|\mathbf{p}\|^3 \\ &\leq -\alpha(1 - \rho) \|\mathbf{g}\| \|\mathbf{p}\| + \frac{L_2\alpha^3 s}{6} \|\mathbf{g}\| \|\mathbf{p}\|^2 \\ &\leq \alpha \|\mathbf{p}\| \|\mathbf{g}\| \left( -(1 - \rho) + \frac{L_2\alpha^2 (s_{\max}^{\text{NC}})}{6} \|\mathbf{p}\| \right), \end{aligned}$$

which implies (7) if

$$\alpha \leq \sqrt{\frac{6(1-\rho)}{L_2 s_{\max}^{\text{NC}} \|\mathbf{p}\|}}, \quad (16)$$

This analysis demonstrates the importance of separating the nonnegative and negative cases. In particular, in the case of the former, the condition  $\alpha \leq 1$  is necessary, while in the latter, the second-order term is omitted entirely, allowing for unrestricted step sizes. This distinction explains why large step sizes (e.g., from forward tracking line search) are feasible in the negative curvature case.

The bounds in (15) and (16) ensure that the line search condition is satisfied by small enough step sizes. While these bounds are typically utilized for proving global convergence, we instead establish a *local unit step size* result for our Hessian-aware scaled gradient descent. Specifically, these bounds imply that, for  $\|\mathbf{p}\|$  sufficiently small, the line search condition (7) is satisfied with  $\alpha = 1$ . Through Proposition 2.2, this can be linked to a condition on the gradient, which forms the proof of Proposition 3.2.

*Proof of Proposition 3.2.* Suppose  $\langle \mathbf{g}, \mathbf{H}\mathbf{g} \rangle \geq 0$ . Since  $s \leq 1/\sigma$ , we have  $\|\mathbf{p}\| \leq \|\mathbf{g}\|/\sigma$  so that if (9) holds then

$$\|\mathbf{p}\| \leq \frac{\|\mathbf{g}\|}{\sigma} \leq \frac{6\sigma(1/2 - \rho)}{L_2},$$

which implies (15) holds with  $\alpha = 1$ . When  $\langle \mathbf{g}, \mathbf{H}\mathbf{g} \rangle < 0$ , we have  $s \leq s_{\max}^{\text{NC}}$ , and hence if (9) then

$$\|\mathbf{p}\| \leq s_{\max}^{\text{NC}} \|\mathbf{g}\| \leq \frac{6(1-\rho)}{L_2 s_{\max}^{\text{NC}}},$$

which implies (16) with  $\alpha = 1$ . □

### B.3. Proof of Theorem 3.5

Let us first restate Theorem 3.5 with all the details and underlying constants.

**Theorem B.1** (Restatement of Theorem 3.5). *Consider Assumptions 3.1 and 3.3 and suppose  $-\infty < f^* = \min_{\mathbf{x} \in \mathbb{R}^d} f(\mathbf{x})$ . For any  $0 < \varepsilon_g < 1$ , after at most*

$$K = \left\lceil \frac{f(\mathbf{x}_0) - f^*}{\min\{c^{\text{SPC}}, c^{\text{LPC}}, c^{\text{NC}}\} \varepsilon_g^2} \right\rceil,$$

*iterations of Algorithm 2, we have  $\|\mathbf{g}_k\| \leq \varepsilon_g$ , where  $c^{\text{SPC}}$ ,  $c^{\text{LPC}}$  and  $c^{\text{NC}}$  are defined as follows:*

$$\begin{aligned} c^{\text{SPC}} &\triangleq \sigma \rho \min \left\{ \left( \frac{6\sigma(\frac{1}{2} - \rho)}{L_2} \right)^2, \frac{1}{L_1^2} \right\} \\ c^{\text{LPC}} &\triangleq \rho \min \left\{ s_{\min}^{\text{LPC}}, \sqrt{\frac{6\sigma(\frac{1}{2} - \rho) s_{\min}^{\text{LPC}}}{L_2}} \right\}, \\ c^{\text{NC}} &\triangleq \rho \sqrt{\frac{6(1-\rho) s_{\min}^{\text{NC}}}{L_2 s_{\max}^{\text{NC}}}}. \end{aligned}$$

Before providing the proof, we note that, as discussed earlier,  $L_1$  and  $L_2$  are lower bounds for the global Lipschitz constants of the problem (if such constants exist), so the factor based on  $L_1$  and  $L_2$  could be significantly smaller than those based on their global counterparts. The constant factor in Theorem B.1 depends quadratically on both  $L_1$  and  $L_2$ , but the dependence on  $L_1$  can be improved to linear if the MR scaling is not used; see Remark B.4. This would align with the dependence on the Lipschitz gradient constant for standard gradient descent in the nonconvex setting.

To prove Theorem B.1, we first consider a lemma which analyzes the worst case *per-iteration* descent for the NC, LPC, and SPC separately.



**Lemma B.2** (Per-iteration Descent). *Consider Assumption 3.1, and let  $\mathbf{p}$  and  $\alpha > 0$  be generated by Algorithm 2. If  $\langle \mathbf{g}, \mathbf{H}\mathbf{g} \rangle < 0$  (NC), then*

$$f(\mathbf{x} + \alpha\mathbf{p}) \leq f(\mathbf{x}) - \rho \sqrt{\frac{6(1-\rho)s_{\min}^{\text{NC}}}{L_2 s_{\max}^{\text{NC}}}} \|\mathbf{g}\|^{3/2}.$$

If  $0 \leq \langle \mathbf{g}, \mathbf{H}\mathbf{g} \rangle \leq \sigma \|\mathbf{g}\|^2$  (LPC), then

$$f(\mathbf{x} + \alpha\mathbf{p}) \leq f(\mathbf{x}) - \rho \min \left\{ s_{\min}^{\text{LPC}} \|\mathbf{g}\|^2, \sqrt{\frac{6\sigma(1/2 - \rho)s_{\min}^{\text{LPC}}}{L_2}} \|\mathbf{g}\|^{3/2} \right\}.$$

Suppose  $\langle \mathbf{g}, \mathbf{H}\mathbf{g} \rangle > \sigma \|\mathbf{g}\|^2$  (SPC). If

$$\|\mathbf{p}\| \geq \frac{6\sigma(1/2 - \rho)}{L_2}, \tag{17}$$

then

$$f(\mathbf{x} + \alpha\mathbf{p}) \leq f(\mathbf{x}) - \rho\sigma \left( \frac{6\sigma(1/2 - \rho)}{L_2} \right)^2.$$

Otherwise, we have  $\alpha = 1$  and

$$f(\mathbf{x} + \mathbf{p}) \leq f(\mathbf{x}) - \rho \|\mathbf{p}\| \|\mathbf{g}\|.$$

*Proof.* (NC) From (16), it follows that the largest step size satisfying (7) must satisfy

$$\alpha \geq \sqrt{\frac{6(1-\rho)}{L_2 s_{\max}^{\text{NC}} \|\mathbf{p}\}}}.$$

Hence,

$$f(\mathbf{x} + \alpha\mathbf{p}) - f(\mathbf{x}) \leq \rho\alpha \langle \mathbf{p}, \mathbf{g} \rangle = -\rho\alpha \|\mathbf{p}\| \|\mathbf{g}\| \leq -\rho \sqrt{\frac{6(1-\rho) \|\mathbf{p}\|}{L_2 s_{\max}^{\text{NC}}}} \|\mathbf{g}\|.$$

Applying  $\|\mathbf{p}\| \geq s_{\min}^{\text{NC}} \|\mathbf{g}\|$  gives the result.

(LPC) Similarly, (15) implies that the largest step size  $\alpha \in (0, 1]$  satisfying (7) must satisfy

$$\alpha \geq \min \left\{ 1, \sqrt{\frac{6\sigma(1/2 - \rho)}{L_2 \|\mathbf{p}\|}} \right\}.$$

Now, from (7) we obtain

$$\begin{aligned} f(\mathbf{x} + \alpha\mathbf{p}) - f(\mathbf{x}) &\leq \rho\alpha \langle \mathbf{p}, \mathbf{g} \rangle = -\rho\alpha \|\mathbf{p}\| \|\mathbf{g}\| \\ &\leq -\rho \min \left\{ \|\mathbf{p}\| \|\mathbf{g}\|, \sqrt{\frac{6\sigma(1/2 - \rho) \|\mathbf{p}\|}{L_2}} \|\mathbf{g}\| \right\}. \end{aligned}$$

Since  $s^{\text{LPC}} \geq s_{\min}^{\text{LPC}}$ ,  $\|\mathbf{p}\| \geq s_{\min}^{\text{LPC}} \|\mathbf{g}\|$ , which yields the result.

(SPC) Similar to the LPC case, (15) implies that the largest step size  $\alpha \in (0, 1]$  satisfying (7) must satisfy

$$\min \left\{ 1, \sqrt{\frac{6\sigma(1/2 - \rho)}{L_2 \|\mathbf{p}\|}} \right\} \leq \alpha \leq 1.$$

Suppose (17) holds, which implies

$$\alpha \geq \sqrt{\frac{6\sigma(1/2 - \rho)}{L_2 \|\mathbf{p}\|}}.$$

In light of (3) and (7) and the fact that  $\langle \mathbf{p}, \mathbf{H}\mathbf{p} \rangle > \sigma \|\mathbf{p}\|^2$ , we have

$$f(\mathbf{x} + \alpha\mathbf{p}) - f(\mathbf{x}) \leq \rho\alpha \langle \mathbf{p}, \mathbf{g} \rangle \leq -\rho\alpha \langle \mathbf{p}, \mathbf{H}\mathbf{p} \rangle \leq -\rho\alpha\sigma \|\mathbf{p}\|^2 \leq -\rho\sigma \left( \frac{6\sigma(1/2 - \rho)}{L_2} \right)^2,$$

where the final inequality follows from (17). If (17) does not hold, then  $\alpha = 1$  and hence

$$f(\mathbf{x} + \mathbf{p}) - f(\mathbf{x}) \leq \rho \langle \mathbf{p}, \mathbf{g} \rangle = -\rho \|\mathbf{g}\| \|\mathbf{p}\|.$$

□

By inspecting the proof of Lemma B.2, we see that the per iteration decrease is independent of the scaling magnitude in all cases except SPC,  $\alpha = 1$ . As discussed in the main body, we handle this case with a regularity condition on the Hessian-gradient product, Assumption 3.3. In particular, Combining (5),  $\sigma \|\mathbf{g}\|^2 < \langle \mathbf{g}, \mathbf{H}\mathbf{g} \rangle$ , and  $\|\mathbf{H}\mathbf{g}\| \leq L_1 \|\mathbf{g}\|$  from Assumption 3.3, we can obtain a lower bound on the SPC scalings.

**Lemma B.3** (Scaling Lower Bounds). *Consider Assumption 3.3 and let  $\sigma \leq L_1$ . We have*

$$\frac{\sigma}{L_1^2} \leq s^{MR} \leq s^{GM} \leq s^{CG}. \quad (18)$$

*Remark B.4.* Note that since  $\langle \mathbf{g}, \mathbf{H}\mathbf{g} \rangle \leq \|\mathbf{H}\mathbf{g}\| \|\mathbf{g}\| \leq L_1 \|\mathbf{g}\|^2$ , the SPC case is detected only when  $\sigma$  is chosen such that  $\sigma \leq L_1$ ; otherwise Algorithm 1 always returns either of LPC or NC scalings. Additionally, by applying  $\|\mathbf{H}\mathbf{g}\| \leq L_1 \|\mathbf{g}\|$  directly to  $s^{GM}$  we can sharpen the lower bound for the CG and GM scalings to  $1/L_1 \leq s^{GM} \leq s^{CG}$ .

With Lemma B.2 and Lemma B.3 in hand, the proof of Theorem 3.5 proceeds by combining the worst case analysis of each case and Lemma B.3.

*Proof of Theorem B.1.* Suppose that  $\|\mathbf{g}_k\| \leq \varepsilon_g$  fails to hold for  $k = 0, \dots, K - 1$ . We divide the iterations  $\mathcal{K} = \{0, \dots, K - 1\}$  into a disjoint union  $\mathcal{K} = \mathcal{K}_{\text{NC}} \cup \mathcal{K}_{\text{LPC}} \cup \mathcal{K}_{\text{SPC}}$  where

$$\begin{aligned} \mathcal{K}_{\text{NC}} &= \{k \in \mathcal{K} \mid \langle \mathbf{g}_k, \mathbf{H}_k \mathbf{g}_k \rangle < 0\} \\ \mathcal{K}_{\text{LPC}} &= \left\{ k \in \mathcal{K} \mid 0 \leq \langle \mathbf{g}_k, \mathbf{H}_k \mathbf{g}_k \rangle \leq \sigma \|\mathbf{g}_k\|^2 \right\} \\ \mathcal{K}_{\text{SPC}} &= \left\{ k \in \mathcal{K} \mid \langle \mathbf{g}_k, \mathbf{H}_k \mathbf{g}_k \rangle > \sigma \|\mathbf{g}_k\|^2 \right\}. \end{aligned}$$

For  $k \in \mathcal{K}_{\text{NC}}$ , Lemma B.2,  $\|\mathbf{g}_k\| > \varepsilon_g$  and  $\varepsilon_g < 1$  give

$$f(\mathbf{x}_k) - f(\mathbf{x}_{k+1}) > \rho \sqrt{\frac{6(1 - \rho)s_{\min}^{\text{NC}}}{L_2 s_{\max}^{\text{NC}}}} \varepsilon_g^{3/2} \geq c^{\text{NC}} \varepsilon_g^2,$$

Similarly, for  $k \in \mathcal{K}_{\text{LPC}}$ , Lemma B.2,  $\|\mathbf{g}_k\| > \varepsilon_g$ , and  $\varepsilon_g < 1$  imply

$$\begin{aligned} f(\mathbf{x}_k) - f(\mathbf{x}_{k+1}) &> \rho \min \left\{ s_{\min}^{\text{LPC}} \|\mathbf{g}_k\|^2, \sqrt{\frac{6\sigma(1/2 - \rho)s_{\min}^{\text{LPC}}}{L_2}} \|\mathbf{g}_k\|^{3/2} \right\} \\ &> \rho \min \left\{ s_{\min}^{\text{LPC}} \varepsilon_g^2, \sqrt{\frac{6\sigma(1/2 - \rho)s_{\min}^{\text{LPC}}}{L_2}} \varepsilon_g^{3/2} \right\} \\ &\geq c^{\text{LPC}} \varepsilon_g^2, \end{aligned}$$

For  $k \in \mathcal{K}_{\text{SPC}}$ , if (17) does not hold, then Lemmas B.2 and B.3 give

$$f(\mathbf{x}_k) - f(\mathbf{x}_{k+1}) \geq \rho \|\mathbf{p}_k\| \|\mathbf{g}_k\| \geq \frac{\sigma\rho}{L_1^2} \|\mathbf{g}_k\|^2 > \frac{\sigma\rho}{L_1^2} \varepsilon_g^2.$$

We can combine this with the case where (17) is satisfied to obtain

$$\begin{aligned} f(\mathbf{x}_k) - f(\mathbf{x}_{k+1}) &> \rho \min \left\{ \sigma \left( \frac{6\sigma^2(1/2 - \rho)}{L_2} \right)^2, \frac{\sigma}{L_1^2} \varepsilon_g^2 \right\} \\ &\geq \sigma\rho \min \left\{ \left( \frac{6\sigma(1/2 - \rho)}{L_2} \right)^2, \frac{1}{L_1^2} \right\} \varepsilon_g^2 \\ &= c^{\text{SPC}} \varepsilon_g^2, \end{aligned}$$

where in the second line we applied  $\varepsilon_g < 1$ . Finally, we apply a telescoping sum over each case

$$\begin{aligned} f(\mathbf{x}_0) - f(\mathbf{x}_K) &= \sum_{i=0}^{K-1} f(\mathbf{x}_i) - f(\mathbf{x}_{i+1}) \\ &= \sum_{k \in \mathcal{K}_{\text{NC}}} f(\mathbf{x}_k) - f(\mathbf{x}_{k+1}) + \sum_{k \in \mathcal{K}_{\text{LPC}}} f(\mathbf{x}_k) - f(\mathbf{x}_{k+1}) + \sum_{k \in \mathcal{K}_{\text{SPC}}} f(\mathbf{x}_k) - f(\mathbf{x}_{k+1}) \\ &> |\mathcal{K}_{\text{NC}}| c^{\text{NC}} \varepsilon_g^2 + |\mathcal{K}_{\text{LPC}}| c^{\text{LPC}} \varepsilon_g^2 + |\mathcal{K}_{\text{SPC}}| c^{\text{SPC}} \varepsilon_g^2 \\ &\geq (|\mathcal{K}_{\text{NC}}| + |\mathcal{K}_{\text{LPC}}| + |\mathcal{K}_{\text{SPC}}|) \min \{c^{\text{NC}}, c^{\text{LPC}}, c^{\text{SPC}}\} \varepsilon_g^2 \\ &= K \min \{c^{\text{NC}}, c^{\text{LPC}}, c^{\text{SPC}}\} \varepsilon_g^2 \\ &\geq f(\mathbf{x}_0) - f^*, \end{aligned}$$

which implies  $f^* > f(\mathbf{x}_K)$ , leading to a contradiction.  $\square$

#### B.4. Proof of Theorem 3.6

We begin with a lemma, which bounds on the objective function sub-optimality and the gradient norm in a region local to a second order sufficient minima.

**Lemma B.5.** *Suppose that  $\mathbf{x}^*$  satisfies the second order sufficient conditions. Furthermore, suppose that  $r$  is chosen such that (10) holds for any  $\mathbf{x} \in \mathcal{B}_r^*$ , then*

$$\frac{\mu}{2} \|\mathbf{x} - \mathbf{x}^*\|^2 \leq f(\mathbf{x}) - f(\mathbf{x}^*) \leq \frac{M}{2} \|\mathbf{x} - \mathbf{x}^*\|^2, \quad (19)$$

$$f(\mathbf{x}) - f(\mathbf{x}^*) \leq \frac{1}{2\mu} \|\mathbf{g}\|^2, \quad (20)$$

$$\mu \|\mathbf{x} - \mathbf{x}^*\| \leq \|\mathbf{g}(\mathbf{x})\| \leq M \|\mathbf{x} - \mathbf{x}^*\|. \quad (21)$$

*Proof.* For any  $\mathbf{x}, \mathbf{y} \in \mathbb{R}^d$ , the mean value theorem for twice differentiable functions implies

$$f(\mathbf{y}) = f(\mathbf{x}) + \langle \mathbf{g}(\mathbf{x}), \mathbf{y} - \mathbf{x} \rangle + \frac{1}{2} \langle \mathbf{y} - \mathbf{x}, \mathbf{H}(\mathbf{x} + t(\mathbf{y} - \mathbf{x}))(\mathbf{y} - \mathbf{x}) \rangle,$$

for some  $t \in (0, 1)$ . If  $\mathbf{x}, \mathbf{y} \in \mathcal{B}_r^*$ , then  $\mathbf{x} + t(\mathbf{y} - \mathbf{x}) \in \mathcal{B}_r^*$ , and so

$$\frac{\mu}{2} \|\mathbf{y} - \mathbf{x}\|^2 \leq f(\mathbf{y}) - f(\mathbf{x}) - \langle \mathbf{g}(\mathbf{x}), \mathbf{y} - \mathbf{x} \rangle \leq \frac{M}{2} \|\mathbf{y} - \mathbf{x}\|^2.$$

By setting  $\mathbf{x} = \mathbf{x}^*$  and  $\mathbf{y} = \mathbf{x} \in \mathcal{B}_r^*$  we obtain (19). Now, by rearranging we obtain

$$f(\mathbf{y}) \geq f(\mathbf{x}) + \langle \mathbf{g}(\mathbf{x}), \mathbf{y} - \mathbf{x} \rangle + \frac{\mu}{2} \|\mathbf{y} - \mathbf{x}\|^2.$$

Minimizing both sides over  $\mathcal{B}_r^*$  gives (20) since

$$\begin{aligned} f(\mathbf{x}^*) &= \min_{\mathbf{y} \in \mathcal{B}_r^*} f(\mathbf{y}) \geq \min_{\mathbf{y} \in \mathcal{B}_r^*} f(\mathbf{x}) + \langle \mathbf{g}(\mathbf{x}), \mathbf{y} - \mathbf{x} \rangle + \frac{\mu}{2} \|\mathbf{y} - \mathbf{x}\|^2 \\ &\geq \min_{\mathbf{y} \in \mathbb{R}^d} f(\mathbf{x}) + \langle \mathbf{g}(\mathbf{x}), \mathbf{y} - \mathbf{x} \rangle + \frac{\mu}{2} \|\mathbf{y} - \mathbf{x}\|^2 \\ &= f(\mathbf{x}) - \frac{1}{2\mu} \|\mathbf{g}(\mathbf{x})\|^2. \end{aligned}$$

Finally, recall that for twice continuously differentiable functions we have

$$\mathbf{g}(\mathbf{x}) = \int_0^1 \mathbf{H}(\mathbf{x}^* + t(\mathbf{x} - \mathbf{x}^*)) (\mathbf{x} - \mathbf{x}^*) dt.$$

Hence, for  $\mathbf{x} \in \mathcal{B}_r^*$ , we get

$$\begin{aligned} \|\mathbf{g}(\mathbf{x})\|^2 &= \langle \mathbf{g}(\mathbf{x}), \mathbf{g}(\mathbf{x}) \rangle = \left\langle \int_0^1 \mathbf{H}(\mathbf{x}^* + t(\mathbf{x} - \mathbf{x}^*)) (\mathbf{x} - \mathbf{x}^*) dt, \int_0^1 \mathbf{H}(\mathbf{x}^* + s(\mathbf{x} - \mathbf{x}^*)) (\mathbf{x} - \mathbf{x}^*) ds \right\rangle \\ &= \int_0^1 \int_0^1 \langle \mathbf{H}(\mathbf{x}^* + t(\mathbf{x} - \mathbf{x}^*)) (\mathbf{x} - \mathbf{x}^*), \mathbf{H}(\mathbf{x}^* + s(\mathbf{x} - \mathbf{x}^*)) (\mathbf{x} - \mathbf{x}^*) \rangle ds dt \\ &= \int_0^1 \int_0^1 \langle \mathbf{x} - \mathbf{x}^*, \mathbf{H}(\mathbf{x}^* + t(\mathbf{x} - \mathbf{x}^*)) \mathbf{H}(\mathbf{x}^* + s(\mathbf{x} - \mathbf{x}^*)) (\mathbf{x} - \mathbf{x}^*) \rangle ds dt. \end{aligned}$$

For positive definite matrices  $\mathbf{A}$  and  $\mathbf{B}$ , we have  $\lambda_{\min}(\mathbf{A})\lambda_{\min}(\mathbf{B}) \leq \lambda_{\min}(\mathbf{AB})$  and  $\lambda_{\max}(\mathbf{AB}) \leq \lambda_{\max}(\mathbf{A})\lambda_{\max}(\mathbf{B})$ . Now since  $t, s \in [0, 1]$  we have

$$\mu^2 \mathbf{I} \preceq \mathbf{H}(\mathbf{x}^* + t(\mathbf{x} - \mathbf{x}^*)) \mathbf{H}(\mathbf{x}^* + s(\mathbf{x} - \mathbf{x}^*)) \preceq M^2 \mathbf{I},$$

which gives the bounds in (21).  $\square$

With Lemma B.5 in hand we prove Theorem 3.6.

*Proof of Theorem 3.6.* Since  $\mathbf{g}(\mathbf{x}^*) = 0$  and the gradient is continuous, we can choose  $r' \leq r$  small enough that that (9) and (10) hold on  $\mathbf{x} \in \mathcal{B}_{r'}^*$ . Now suppose that  $\mathbf{x}_k \in \mathcal{B}_{r'}^*$ , Proposition 3.2 and (7) and (20) imply

$$f(\mathbf{x}_{k+1}) \leq f(\mathbf{x}_k) + \rho \langle \mathbf{p}_k, \mathbf{g}_k \rangle = f(\mathbf{x}_k) - s_k \rho \|\mathbf{g}_k\|^2 \leq f(\mathbf{x}_k) - 2s_k \mu \rho (f(\mathbf{x}_k) - f(\mathbf{x}^*)),$$

which implies

$$f(\mathbf{x}_{k+1}) - f(\mathbf{x}^*) \leq (1 - 2\mu \rho s_k) (f(\mathbf{x}_k) - f(\mathbf{x}^*)). \quad (22)$$

Since  $\mathbf{H}_k \succ 0$ , we only need to consider LPC and SPC scalings. If  $\mathbf{g}_k$  is a SPC direction, then following a similar line of reasoning as that in Lemma B.3, with  $M$  taking the place of  $L_1$ , we get  $s_k = s^{\text{SPC}} \geq 1/M$ . Note that for the MR scaling, this bound follows from  $\mu \mathbf{I} \preceq \mathbf{H}_k \preceq M \mathbf{I}$  and Lemma C.1. Hence, (22) gives

$$f(\mathbf{x}_{k+1}) - f(\mathbf{x}^*) \leq \left(1 - \frac{2\mu\rho}{M}\right) (f(\mathbf{x}_k) - f(\mathbf{x}^*)). \quad (23)$$

If  $\sigma < \mu$  then clearly  $\mathbf{g}_k$  cannot be an LPC direction and so (23) yields the desired recursion in function sub-optimality. On the other hand, if  $\sigma \geq \mu$  and  $\mathbf{g}_k$  is an LPC direction, then we simply apply  $s_{\min}^{\text{LPC}} \leq s^{\text{LPC}}$  to (22) to obtain

$$f(\mathbf{x}_{k+1}) - f(\mathbf{x}^*) \leq (1 - 2\mu s_{\min}^{\text{LPC}} \rho) (f(\mathbf{x}_k) - f(\mathbf{x}^*)). \quad (24)$$

The desired recursion follows from combining (23) and (24).

It remains to show that the iterates remain in  $\mathcal{B}_{r'}^*$ . To this end, define the set

$$\mathcal{F} = \left\{ x \mid f(\mathbf{x}) - f(\mathbf{x}^*) \leq \frac{\mu\sigma^2 r^2}{2(\sigma + M)^2} \right\}.$$

Now suppose that an iterate  $\mathbf{x}_k$  is sufficiently close to  $\mathbf{x}^*$  such that  $\mathbf{x}_k \in B_{r'}^* \cap \mathcal{F}$ . Such  $\mathbf{x}_k$  exists, as implied by the upper bound in (19). We now show that all subsequent iterates remain in  $B_{r'}^* \cap \mathcal{F}$ . Indeed, from the earlier part of the proof, we get  $f(\mathbf{x}_{k+1}) - f(\mathbf{x}^*) \leq (1 - \tau)(f(\mathbf{x}_k) - f(\mathbf{x}^*))$ , which implies  $\mathbf{x}_{k+1} \in \mathcal{F}$ . On the other hand, from  $\mathbf{x}_{k+1} = \mathbf{x}_k - s_k \mathbf{g}_k$  (since  $\alpha = 1$  is accepted by the line search),  $s \leq 1/\sigma$  (Proposition 2.2), the upper bound in (21), and the lower bound in (19), it follows that

$$\begin{aligned} \|\mathbf{x}_{k+1} - \mathbf{x}^*\| &\leq \|\mathbf{x}_k - \mathbf{x}^*\| + s_k \|\mathbf{g}_k\| \leq \left(1 + \frac{M}{\sigma}\right) \|\mathbf{x}_k - \mathbf{x}^*\| \\ &\leq \left(1 + \frac{M}{\sigma}\right) \sqrt{\frac{2}{\mu}} (f(\mathbf{x}_k) - f(\mathbf{x}^*)) \leq r, \end{aligned}$$

which gives  $\mathbf{x}_{k+1} \in B_{r'}^*$ , and hence  $\mathbf{x}_{k+1} \in B_{r'}^* \cap \mathcal{F}$ .  $\square$

### B.5. Convergence in Gradient Norm and Proof of Theorem 3.8

We prove Theorem 3.8 by considering a more general result, Proposition B.9, to which Theorem 3.8 is a corollary. Our analysis begins by utilizing Assumption 3.1 and a bound on the residual to obtain a recursion in the gradient norm.

**Lemma B.6.** *Considering Assumption 3.1 and supposing  $\|\mathbf{H}\mathbf{g}\| \neq 0$  and  $\|\mathbf{g}\| \neq 0$  we have the following recursion for the gradient with the step  $\mathbf{p} = -s^{\text{MR}}\mathbf{g}$*

$$\|\mathbf{g}(\mathbf{x} + \mathbf{p})\| \leq \frac{L_2}{2} \|\mathbf{p}\|^2 + \sqrt{1 - \cos^2 \theta} \|\mathbf{g}\|, \quad (25)$$

where  $\theta \triangleq \angle(\mathbf{g}, \mathbf{H}\mathbf{g})$  is the angle between  $\mathbf{g}$  and  $\mathbf{H}\mathbf{g}$ .

*Proof.* Adding and subtracting appropriate values and applying the triangle inequality we have

$$\begin{aligned} \|\mathbf{g}(\mathbf{x} + \mathbf{p})\| &= \|\mathbf{g}(\mathbf{x} + \mathbf{p}) + \mathbf{g} + \mathbf{H}\mathbf{p} - \mathbf{g} - \mathbf{H}\mathbf{p}\| \\ &\leq \|\mathbf{g}(\mathbf{x} + \mathbf{p}) - \mathbf{g} - \mathbf{H}\mathbf{p}\| + \|\mathbf{g} + \mathbf{H}\mathbf{p}\| \\ &= \|\mathbf{g}(\mathbf{x} + \mathbf{p}) - \mathbf{g} - \mathbf{H}\mathbf{p}\| + \|\mathbf{r}\|. \end{aligned}$$

Now, Assumption 3.1 and (13) gives

$$\|\mathbf{g}(\mathbf{x} + \mathbf{p})\| \leq \frac{L_2}{2} \|\mathbf{p}\|^2 + \|\mathbf{r}\|.$$

We can handle the residual term using the properties of MR scaling. Indeed, applying the definition of  $s^{\text{MR}}$  for  $\mathbf{H}\mathbf{g} \neq 0$  we have

$$\begin{aligned} \|\mathbf{r}\|^2 &= \|\mathbf{g} - s^{\text{MR}}\mathbf{H}\mathbf{g}\|^2 = \|\mathbf{g}\|^2 - 2s^{\text{MR}} \langle \mathbf{g}, \mathbf{H}\mathbf{g} \rangle + (s^{\text{MR}})^2 \|\mathbf{H}\mathbf{g}\|^2 \\ &= \|\mathbf{g}\|^2 - 2 \frac{\langle \mathbf{g}, \mathbf{H}\mathbf{g} \rangle^2}{\|\mathbf{H}\mathbf{g}\|^2} + \frac{\langle \mathbf{g}, \mathbf{H}\mathbf{g} \rangle^2}{\|\mathbf{H}\mathbf{g}\|^2} \\ &= \|\mathbf{g}\|^2 \left(1 - \frac{\langle \mathbf{g}, \mathbf{H}\mathbf{g} \rangle^2}{\|\mathbf{H}\mathbf{g}\|^2 \|\mathbf{g}\|^2}\right) \\ &= \|\mathbf{g}\|^2 (1 - \cos^2 \theta), \end{aligned}$$

Putting this all together yields

$$\|\mathbf{g}(\mathbf{x} + \mathbf{p})\| \leq \frac{L_2}{2} \|\mathbf{p}\|^2 + \sqrt{1 - \cos^2 \theta} \|\mathbf{g}\|.$$

which is (25).  $\square$

To apply (25) for convergence in gradient norm, the magnitude of  $(s^{\text{MR}})^2$  needs to be bounded from above and  $\cos \theta$  must remain bounded away from zero. To that end, we introduce Assumption B.7, which excludes cases where the MR scaling becomes unbounded and  $\theta \approx \pi/2$ , meaning  $\mathbf{H}\mathbf{g}$  and  $\mathbf{g}$  become nearly orthogonal.

**Assumption B.7.** Given  $\mathbf{x}_0$ , there exists constants  $\nu_0 > 0$  and  $\mu_0 > 0$ , possibly depending on  $\mathbf{x}_0$ , such that for all the iterates of the form  $\mathbf{x}_{k+1} = \mathbf{x}_k - s_k^{\text{MR}} \mathbf{g}_k$ ,  $k \geq 0$ , with  $\mathbf{g}_k \neq 0$  we have

$$\mu_0 \|\mathbf{g}_k\|^2 \leq |\langle \mathbf{g}_k, \mathbf{H}_k \mathbf{g}_k \rangle|, \quad (26)$$

$$\nu_0 \leq \cos^2 \theta_k. \quad (27)$$

*Remark B.8.* The conditions in Assumption B.7 are general and somewhat unconventional. However, as we shall see they are a weakening of more typical conditions. Indeed, any smooth and strongly convex function on the set containing the iterates satisfies Assumption B.7. Furthermore, as we shall see in the proof of Theorem 3.8, the second order sufficient conditions subsume Assumption B.7 for  $\mathbf{x}_0$  close enough to a minima. The gradient curvature condition, (26), is a weakening of strong convexity, as the curvature along gradient direction need only be uniformly bounded away from zero (instead of uniformly positive). Applying the Cauchy-Schwarz inequality to (26) we see that  $\|\mathbf{g}_k\| > 0$  implies  $\|\mathbf{H}_k \mathbf{g}_k\| > 0$ , which ensures that  $\cos \theta_k$  and  $s_k^{\text{MR}}$  remain well defined along the path of the iterates. On the other hand, the cosine condition (27) is implied by (26) along with a bound of the form  $\|\mathbf{H}_k \mathbf{g}_k\| \leq L \|\mathbf{g}_k\|$ . However, (27) is also more generally applicable. For example, when  $d = 1$ , (27) holds with  $\cos^2 \theta = 1$ , so long as  $\mathbf{H} \neq 0$ . Another example, is  $f(\mathbf{x}) = \|\mathbf{x}\|^3 / 6$  where, again, one can show  $\cos^2 \theta = 1$ .

An immediate consequence of (26) and  $\|\mathbf{H}_k \mathbf{g}_k\| \geq |\langle \mathbf{g}_k, \mathbf{H}_k \mathbf{g}_k \rangle| / \|\mathbf{g}_k\|$  is that

$$(s_k^{\text{MR}})^2 = \frac{(\langle \mathbf{g}_k, \mathbf{H}_k \mathbf{g}_k \rangle)^2}{\|\mathbf{H}_k \mathbf{g}_k\|^4} \leq \frac{\|\mathbf{g}_k\|^4}{(\langle \mathbf{g}_k, \mathbf{H}_k \mathbf{g}_k \rangle)^2} \leq \frac{1}{\mu_0^2}.$$

Therefore by applying Assumption B.7 and (25), we get

$$\|\mathbf{g}(\mathbf{x} + \mathbf{p})\| \leq \left( \frac{L_2}{2\mu_0^2} \|\mathbf{g}\| + \sqrt{1 - \nu_0} \right) \|\mathbf{g}\|. \quad (28)$$

The recursion in the gradient norm, (28), is linear-quadratic in a manner similar to the results obtained for Newton-MR method applied to invex problems; see (Roosta et al., 2022). It follows directly from (28) that, when the gradient is small enough, i.e.,

$$\|\mathbf{g}\| < G_0 \triangleq 2\mu_0^2 (1 - \sqrt{1 - \nu_0}) / L_2, \quad (29)$$

the gradient norm decreases monotonically. Naturally, once the gradient hits this monotonic phase, every subsequent iterate will also satisfy  $\|\mathbf{g}\| \leq G_0$ . These properties are all formalized to a rate in Proposition B.9.

**Proposition B.9** (MR Scaling Convergence Gradient Norm). *Consider Assumption 3.1, and iterations of the form  $\mathbf{x}_{k+1} = \mathbf{x}_k - s_k^{\text{MR}} \mathbf{g}_k$  starting from  $\mathbf{x}_0$  for which  $\|\mathbf{g}(\mathbf{x}_0)\| < G_0$  and Assumption B.7 holds. For all  $k \geq 1$ , we have  $\|\mathbf{g}_k\| < \|\mathbf{g}_{k-1}\|$  and*

$$\|\mathbf{g}_k\| \leq \frac{G_0}{G_0 - \|\mathbf{g}_0\|} \left( 1 - \frac{1 - \sqrt{1 - \nu_0}}{2 - \sqrt{1 - \nu_0}} \right)^k \|\mathbf{g}_0\|.$$

*Proof.* Since Assumption B.7 holds with  $\mathbf{x}_0$  and  $\|\mathbf{g}(\mathbf{x}_0)\| < G_0$ , (28) implies that  $\|\mathbf{g}_k\| \leq \|\mathbf{g}_{k-1}\| < G_0$  for  $k \geq 1$ . To obtain a quantitative rate, we follow a similar line of reasoning as (Nesterov, 2004, Theorem 1.2.4). Let  $a_k = \|\mathbf{g}_k\| L_2 / (2\mu_0^2)$  and  $q = 1 - \sqrt{1 - \nu_0}$ . We have  $a_k < q$  and

$$a_{k+1} \leq a_k^2 + \sqrt{1 - \nu_0} a_k = (a_k + \sqrt{1 - \nu_0}) a_k = (1 + a_k - q) a_k.$$

Also, since  $a_k - q < 0$  by (29),

$$a_k (1 + a_k - q) = \left( \frac{(1 - (a_k - q))(1 + (a_k - q))}{(1 - (a_k - q))} \right) a_k = \left( \frac{(1 - (a_k - q)^2)}{1 - (a_k - q)} \right) a_k \leq \frac{a_k}{1 + q - a_k},$$

where the inequality follows from  $(1 - (a_k - q)^2) \leq 1$ . Hence,

$$\frac{q}{a_{k+1}} - 1 \geq (1 + q) \left( \frac{q}{a_k} - 1 \right).$$

Applying this iteratively gives

$$\frac{q}{a_k} - 1 \geq (1+q)^k \left( \frac{q}{a_0} - 1 \right) = (1+q)^k \left( \frac{2\mu_0^2(1-\sqrt{1-\nu_0})}{L_2 \|\mathbf{g}_0\|} - 1 \right) = (1+q)^k \left( \frac{G_0}{\|\mathbf{g}_0\|} - 1 \right).$$

Rearranging, we obtain

$$a_k \leq \frac{q \|\mathbf{g}_0\|}{(1+q)^k (G_0 - \|\mathbf{g}_0\|) + \|\mathbf{g}_0\|}.$$

Finally, by substituting in the definition of  $a_k$  and  $q$ , we obtain

$$\|\mathbf{g}_k\| \leq \frac{G_0 \|\mathbf{g}_0\|}{(2 - \sqrt{1 - \nu_0})^k (G_0 - \|\mathbf{g}_0\|)} = \frac{G_0}{G_0 - \|\mathbf{g}_0\|} \left( 1 - \frac{1 - \sqrt{1 - \nu_0}}{2 - \sqrt{1 - \nu_0}} \right)^k \|\mathbf{g}_0\|.$$

□

Finally, we prove Theorem 3.8 by specializing to the case where the second order sufficient conditions hold.

*Proof of Theorem 3.8.* It suffices to find a region where the conditions of Proposition B.9 are satisfied, that the iterates will not leave. Similar to the proof of Theorem 3.6, when the second order sufficient conditions hold, there exists a ball  $\mathcal{B}_r^*$  such that (10) holds. This in turn implies (21), as well as (26) and (27) with  $\mu_0 = \mu$  and  $\nu_0 = \mu^2/M^2$ , respectively, for any  $\mathbf{x} \in \mathcal{B}_r^*$ . With these  $\mu_0$  and  $\nu_0$  in hand, consider  $G_0$  in (29) and define

$$\mathcal{G} = \left\{ \mathbf{x} \mid 0 < \|\mathbf{g}(\mathbf{x})\| \leq \min \left\{ G_0, \frac{r\mu}{M\mu + 1} \right\} \right\}.$$

Suppose  $\mathbf{x}_k \in \mathcal{B}_r^* \cap \mathcal{G}$  (such an  $\mathbf{x}_k$  exists by the RHS of (21)). From (28), we get  $\|\mathbf{g}_{k+1}\| < \|\mathbf{g}_k\|$ , which in turn implies  $\mathbf{x}_{k+1} \in \mathcal{G}$ . Applying the upper bound in (21),  $s_k^{\text{MR}} \leq 1/\mu$  and  $\mathbf{x}_k \in \mathcal{G}$ , gives

$$\|\mathbf{x}_{k+1} - \mathbf{x}^*\| \leq \|\mathbf{x}_k - \mathbf{x}^*\| + |s_k^{\text{MR}}| \|\mathbf{g}_k\| \leq \left( M + \frac{1}{\mu} \right) \|\mathbf{g}_k\| \leq r.$$

That is,  $\mathbf{x}_{k+1} \in \mathcal{B}_r^* \cap \mathcal{G}$ . Hence, Assumption B.7 holds for all of the iterates if  $\mathbf{x}_0 \in \mathcal{B}_r^* \cap \mathcal{G}$ . Proposition B.9 can be applied to obtain the convergence rate. □

Finally, we remark that the iteration  $\mathbf{x}_{k+1} = \mathbf{x}_k - s_k^{\text{MR}} \mathbf{g}_k$ , as applied in Theorem 3.8, can occur as a special case of Algorithm 2. In particular, if  $\sigma$  is chosen  $\sigma < \mu$  then the SPC scaling (in particular, the MR scaling) will always be selected. Moreover, if  $\mathbf{x}_0$  is chosen sufficiently close to  $\mathbf{x}^*$ , (9) will hold; implying that  $\alpha = 1$  will be acceptable to the line search. Indeed, (9) will be satisfied for all future iterations by monotonicity of the gradient norm.

## B.6. Inexact Hessian Scaling and Proof of Proposition 3.10 and Proposition 3.12

When running Algorithm 1 with  $\tilde{\mathbf{H}}$  in place of  $\mathbf{H}$  the curvature tolerance tests as well as the scalings (in the SPC case) now depend on  $\tilde{\mathbf{H}}$ . Fortunately, many of the key properties from the deterministic case still hold for inexact Hessian. Indeed, SPC steps satisfy  $\sigma \|\mathbf{g}\|^2 < \langle \mathbf{g}, \tilde{\mathbf{H}} \mathbf{g} \rangle$ , LPC steps satisfy  $0 \leq \langle \mathbf{g}, \tilde{\mathbf{H}} \mathbf{g} \rangle \leq \sigma \|\mathbf{g}\|^2$  and NC steps satisfy  $\langle \mathbf{g}, \tilde{\mathbf{H}} \mathbf{g} \rangle < 0$ . The second order descent condition (3) from Proposition 2.3 continues to hold with respect to  $\tilde{\mathbf{H}}$ , that is,

$$\langle \mathbf{g}, \tilde{\mathbf{p}} \rangle + \langle \tilde{\mathbf{p}}, \tilde{\mathbf{H}} \tilde{\mathbf{p}} \rangle \leq 0, \quad (30)$$

Moreover, the upper bounds from Proposition 2.2 continue to hold, as they arise due to the curvature test. On the other hand, if Assumption 3.11 holds then we have a lower bound (compare with Lemma B.3) on the scaling magnitudes

$$\frac{\sigma}{\bar{L}_1^2} \leq s^{\text{MR}} \leq s^{\text{GM}} \leq s^{\text{CG}}. \quad (31)$$

The search direction,  $\tilde{\mathbf{p}}$ , also remains collinear to the gradient, so that,  $\langle \mathbf{g}, \tilde{\mathbf{p}} \rangle = -\|\mathbf{g}\| \|\tilde{\mathbf{p}}\|$  and (14) can be applied along  $\tilde{\mathbf{p}}$ . The Armijo condition for the line search is given by

$$f(\mathbf{x} + \alpha \tilde{\mathbf{p}}) \leq f(\mathbf{x}) + \alpha \rho \langle \mathbf{g}, \tilde{\mathbf{p}} \rangle, \quad (32)$$

for  $\rho \in (0, 1/2)$ . With these ideas in hand we can derive the results for Section 3.3. Starting with the proof of Proposition 3.10.

**Proof of Proposition 3.10**

*Proof of Proposition 3.10.* We begin by adding and subtracting  $\langle \tilde{\mathbf{p}}, \tilde{\mathbf{H}}\tilde{\mathbf{p}} \rangle$  to the upper bound in (14) and applying Assumption 3.9

$$\begin{aligned} f(\mathbf{x} + \alpha\mathbf{p}) - f(\mathbf{x}) &\leq \alpha \langle \mathbf{g}, \tilde{\mathbf{p}} \rangle + \frac{\alpha^2}{2} \langle \tilde{\mathbf{p}}, (\mathbf{H} - \tilde{\mathbf{H}})\tilde{\mathbf{p}} \rangle + \frac{\alpha^2}{2} \langle \tilde{\mathbf{p}}, \tilde{\mathbf{H}}\tilde{\mathbf{p}} \rangle + \frac{L_2\alpha^3}{6} \|\tilde{\mathbf{p}}\|^3 \\ &\leq \alpha \langle \mathbf{g}, \tilde{\mathbf{p}} \rangle + \frac{\alpha^2\Delta_H}{2} \|\tilde{\mathbf{p}}\|^2 + \frac{\alpha^2}{2} \langle \tilde{\mathbf{p}}, \tilde{\mathbf{H}}\tilde{\mathbf{p}} \rangle + \frac{L_2\alpha^3}{6} \|\tilde{\mathbf{p}}\|^3. \end{aligned} \quad (33)$$

The upper bound in (33) now involves the curvature of the inexact Hessian,  $\langle \tilde{\mathbf{p}}, \tilde{\mathbf{H}}\tilde{\mathbf{p}} \rangle$ , which we can control with the curvature tests and second order descent condition. Starting with non-negative curvature case (encompassing SPC and LPC scalings) with  $\langle \mathbf{g}, \tilde{\mathbf{H}}\mathbf{g} \rangle \geq 0$ . Taking (33), subtracting  $\rho\alpha \langle \mathbf{g}, \tilde{\mathbf{p}} \rangle$  and applying  $\alpha \leq 1$  and (30) we obtain

$$\begin{aligned} f(\mathbf{x} + \alpha\mathbf{p}) - f(\mathbf{x}) - \rho\alpha \langle \mathbf{g}, \tilde{\mathbf{p}} \rangle &\leq \alpha \left( \frac{1}{2} - \rho \right) \langle \mathbf{g}, \tilde{\mathbf{p}} \rangle + \frac{\alpha}{2} \left( \langle \mathbf{g}, \tilde{\mathbf{p}} \rangle + \langle \tilde{\mathbf{p}}, \tilde{\mathbf{H}}\tilde{\mathbf{p}} \rangle \right) + \frac{\alpha^2}{2} \Delta_H \|\tilde{\mathbf{p}}\|^2 + \frac{L_2\alpha^3}{6} \|\tilde{\mathbf{p}}\|^3 \\ &\leq -\alpha \left( \frac{1}{2} - \rho \right) \|\mathbf{g}\| \|\tilde{\mathbf{p}}\| + \frac{\alpha^2}{2} \Delta_H \|\tilde{\mathbf{p}}\|^2 + \frac{L_2\alpha^3}{6} \|\tilde{\mathbf{p}}\|^3 \\ &= \left( -\left( \frac{1}{2} - \rho \right) + \frac{\alpha\tilde{s}\Delta_H}{2} + \frac{L_2\alpha^2\tilde{s}}{6} \|\tilde{\mathbf{p}}\| \right) \alpha \|\tilde{\mathbf{p}}\| \|\mathbf{g}\| \\ &\leq \left( -\left( \frac{1}{2} - \rho \right) + \frac{\alpha\Delta_H}{2\sigma} + \frac{L_2\alpha^2}{6\sigma} \|\tilde{\mathbf{p}}\| \right) \alpha \|\tilde{\mathbf{p}}\| \|\mathbf{g}\|. \end{aligned} \quad (34)$$

In the final line we apply  $\tilde{s} \leq 1/\sigma$ , which holds for both the LPC and SPC scalings. The line search criteria (32) is clearly satisfied if the upper bound in (34) is negative. That is,

$$\|\tilde{\mathbf{p}}\| \leq \frac{6\sigma}{L_2\alpha^2} \left( \left( \frac{1}{2} - \rho \right) - \frac{\alpha\Delta_H}{2\sigma} \right).$$

This bound is nontrivial if

$$\Delta_H \leq \frac{2\sigma}{\alpha} \left( \frac{1}{2} - \rho \right).$$

Now we consider the negative curvature case, where  $\langle \mathbf{g}, \tilde{\mathbf{H}}\mathbf{g} \rangle < 0$ . Applying the negative curvature condition to (33) and subtracting  $\alpha\rho \langle \mathbf{g}, \tilde{\mathbf{p}} \rangle$

$$\begin{aligned} f(\mathbf{x} + \alpha\mathbf{p}) - f(\mathbf{x}) - \alpha\rho \langle \mathbf{g}, \tilde{\mathbf{p}} \rangle &\leq \alpha(1 - \rho) \langle \mathbf{g}, \tilde{\mathbf{p}} \rangle + \frac{\alpha^2\Delta_H}{2} \|\tilde{\mathbf{p}}\|^2 + \frac{\alpha^2}{2} \langle \tilde{\mathbf{p}}, \tilde{\mathbf{H}}\tilde{\mathbf{p}} \rangle + \frac{L_2\alpha^3}{6} \|\tilde{\mathbf{p}}\|^3 \\ &\leq -\alpha(1 - \rho) \|\mathbf{g}\| \|\tilde{\mathbf{p}}\| + \frac{\alpha^2\Delta_H}{2} \|\tilde{\mathbf{p}}\|^2 + \frac{L_2\alpha^3}{6} \|\tilde{\mathbf{p}}\|^3 \\ &= \left( -(1 - \rho) + \frac{\alpha\tilde{s}^{\text{NC}}}{2} \Delta_H + \frac{L_2\alpha^2\tilde{s}^{\text{NC}}}{6} \|\tilde{\mathbf{p}}\| \right) \alpha \|\mathbf{g}\| \|\tilde{\mathbf{p}}\| \\ &\leq \left( -(1 - \rho) + \frac{\alpha s_{\max}^{\text{NC}}}{2} \Delta_H + \frac{L_2\alpha^2 s_{\max}^{\text{NC}}}{6} \|\tilde{\mathbf{p}}\| \right) \alpha \|\mathbf{g}\| \|\tilde{\mathbf{p}}\|, \end{aligned} \quad (35)$$

where in the final line we we apply  $\tilde{s}^{\text{NC}} \leq s_{\max}^{\text{NC}}$ . Again, if the upper bound in (35) is negative (32) is clearly satisfied. In particular, (35) is negative if

$$\|\tilde{\mathbf{p}}\| \leq \frac{6}{L_2 s_{\max}^{\text{NC}} \alpha^2} \left( 1 - \rho - \frac{\alpha s_{\max}^{\text{NC}} \Delta_H}{2} \right).$$

This bound is nontrivial if

$$\Delta_H \leq \frac{2(1 - \rho)}{\alpha s_{\max}^{\text{NC}}}.$$



The result follows from combining the two tolerances on  $\Delta_H$ , setting  $\alpha = 1$  and using the fact that  $\|\tilde{\mathbf{p}}\| \leq \|\mathbf{g}\|/\sigma$  in the non-negative curvature case and  $\|\tilde{\mathbf{p}}\| \leq s_{\max}^{\text{NC}} \|\mathbf{g}\|$  in the negative curvature case.  $\square$

Next we prove the global convergence result in Proposition 3.12.

**Proof of Proposition 3.12** To establish a global convergence rate we need a technical lemma

**Lemma B.10.** For  $A \geq 0$ ,  $x \geq 0$  and  $B > 0$  we have

$$-A + \sqrt{A^2 + Bx} \geq \frac{B}{A + \sqrt{A^2 + B}} \min\{x, 1\}.$$

*Proof.* The  $x = 0$  case is trivial, so take  $x > 0$ . Multiplying the numerator and denominator by a conjugate

$$\begin{aligned} -A + \sqrt{A^2 + Bx} &= \frac{(-A + \sqrt{A^2 + Bx})(A + \sqrt{A^2 + Bx})}{A + \sqrt{A^2 + Bx}} \\ &= \frac{-A^2 + A^2 + Bx}{A + \sqrt{A^2 + Bx}} \\ &= \frac{Bx}{A + \sqrt{A^2 + Bx}}. \end{aligned}$$

Now consider two cases. If  $x < 1$  then  $A + \sqrt{A^2 + Bx} < A + \sqrt{A^2 + B}$  so that

$$-A + \sqrt{A^2 + Bx} = \frac{Bx}{A + \sqrt{A^2 + Bx}} \geq \frac{B}{A + \sqrt{A^2 + B}} x.$$

On the other hand, if  $x \geq 1$ , we rearrange to obtain

$$-A + \sqrt{A^2 + Bx} = \frac{Bx}{A + \sqrt{A^2 + Bx}} = \frac{B}{A/x + \sqrt{A^2/x^2 + B/x}}.$$

The denominator of this expression is decreasing in  $x$ , indeed, we clearly have  $A/x + \sqrt{A^2/x^2 + B/x} \leq A + \sqrt{A^2 + B}$  so that

$$-A + \sqrt{A^2 + Bx} \geq \frac{B}{A + \sqrt{A^2 + B}}.$$

$\square$

*Proof of Proposition 3.12.* We begin by re-examining (34) and (35) from the proof of Proposition 3.10, in terms of  $\alpha$ , to demonstrate that there is a positive step size for which (32) certainly holds. We assume that Algorithm 2 has not terminated, i.e.,  $\|\mathbf{g}\| > \varepsilon_g$ . Starting with the negative curvature case. Consider the upper bound in (35). The line search condition (32) is certainly satisfied if

$$C_2 \alpha^2 + C_1 \alpha + C_0 \leq 0,$$

where

$$C_2 \triangleq \frac{L_2 s_{\max}^{\text{NC}} \|\tilde{\mathbf{p}}\|}{6}, \quad C_1 \triangleq \frac{s_{\max}^{\text{NC}} \Delta_H}{2}, \quad C_0 \triangleq -(1 - \rho).$$

This quadratic has two real roots, one positive and one negative. The positive root is given by

$$\begin{aligned} \alpha_1^* &= -\frac{C_1}{2C_2} + \sqrt{\frac{C_1^2}{4C_2^2} - \frac{C_0}{C_2}} \\ &= -\frac{3\Delta_H}{2L_2 \|\tilde{\mathbf{p}}\|} + \sqrt{\frac{9\Delta_H^2}{4L_2^2 \|\tilde{\mathbf{p}}\|^2} + \frac{6(1 - \rho)}{L_2 s_{\max}^{\text{NC}} \|\tilde{\mathbf{p}}\|}}, \end{aligned}$$

which implies that the largest step size for which (32) is satisfied also must satisfy  $\alpha \geq \alpha_1^*$ . Therefore, when (32) is satisfied, we have

$$\begin{aligned}
 f(\mathbf{x} + \alpha \tilde{\mathbf{p}}) - f(\mathbf{x}) &\leq -\alpha \rho \|\tilde{\mathbf{p}}\| \|\mathbf{g}\| \\
 &\leq -\rho \left( -\frac{3\Delta_H}{2L_2} + \sqrt{\frac{9\Delta_H^2}{4L_2^2} + \frac{6(1-\rho)\|\tilde{\mathbf{p}}\|}{L_2 s_{\max}^{\text{NC}}}} \right) \|\mathbf{g}\| \\
 &< -\rho \left( -\frac{3\Delta_H}{2L_2} + \sqrt{\frac{9\Delta_H^2}{4L_2^2} + \frac{6(1-\rho)s_{\min}^{\text{NC}}\varepsilon_g}{L_2 s_{\max}^{\text{NC}}}} \right) \varepsilon_g \\
 &\leq -\rho \left( \frac{6(1-\rho)s_{\min}^{\text{NC}}/(L_2 s_{\max}^{\text{NC}})}{\frac{3\Delta_H}{2L_2} + \sqrt{\frac{9\Delta_H^2}{4L_2^2} + \frac{6(1-\rho)s_{\min}^{\text{NC}}}{L_2 s_{\max}^{\text{NC}}}}} \right) \varepsilon_g^2 \\
 &= -\tilde{c}^{\text{NC}} \varepsilon_g^2.
 \end{aligned}$$

On the third line we apply  $\|\tilde{\mathbf{p}}\| \geq s_{\min}^{\text{NC}} \|\mathbf{g}\|$  and  $\|\mathbf{g}\| > \varepsilon_g$ , whereas on the fourth line we apply Lemma B.10 and  $\varepsilon_g < 1$ . In the final line we define

$$\tilde{c}^{\text{NC}} \triangleq \rho \frac{12(1-\rho)s_{\min}^{\text{NC}}/s_{\max}^{\text{NC}}}{3\Delta_H + \sqrt{9\Delta_H^2 + 24(1-\rho)L_2 s_{\min}^{\text{NC}}/s_{\max}^{\text{NC}}}}.$$

Next we come to the positive curvature case. Considering (34) we see that the line search condition (32) is satisfied if

$$D_2 \alpha^2 + D_1 \alpha + D_0 \leq 0,$$

where

$$D_2 \triangleq \frac{L_2 \|\tilde{\mathbf{p}}\|}{6\sigma}, \quad D_1 \triangleq \frac{\Delta_H}{2\sigma}, \quad D_0 \triangleq -\left(\frac{1}{2} - \rho\right).$$

Again this quadratic has a positive and negative root. The positive root is given by

$$\begin{aligned}
 \alpha_2^* &\triangleq -\frac{D_1}{2D_2} + \sqrt{\frac{D_1^2}{4D_2^2} - \frac{D_0}{D_2}} \\
 &= -\frac{3\Delta_H}{2L_2 \|\tilde{\mathbf{p}}\|} + \sqrt{\frac{9\Delta_H^2}{4L_2^2 \|\tilde{\mathbf{p}}\|^2} + \frac{6\sigma(1/2 - \rho)}{L_2 \|\tilde{\mathbf{p}}\|}}.
 \end{aligned}$$

Therefore, the largest step size for which (32) holds must satisfy  $\alpha \geq \min\{1, \alpha_2^*\}$ . We now isolate the LPC and SPC cases. For the LPC case, by combining the line search criteria (32) and  $\alpha \geq \min\{1, \alpha_2^*\}$  we obtain

$$\begin{aligned}
 f(\mathbf{x} + \alpha \tilde{\mathbf{p}}) - f(\mathbf{x}) &\leq -\rho \alpha \|\mathbf{g}\| \|\tilde{\mathbf{p}}\| \\
 &\leq -\rho \min\{\alpha_2^* \|\tilde{\mathbf{p}}\|, \|\tilde{\mathbf{p}}\|\} \|\mathbf{g}\| \\
 &= -\rho \min\left\{-\frac{3\Delta_H}{2L_2} + \sqrt{\frac{9\Delta_H^2}{4L_2^2} + \frac{6\sigma(1/2 - \rho)\|\tilde{\mathbf{p}}\|}{L_2}}, \|\tilde{\mathbf{p}}\|\right\} \|\mathbf{g}\| \\
 &< -\rho \min\left\{-\frac{3\Delta_H}{2L_2} + \sqrt{\frac{9\Delta_H^2}{4L_2^2} + \frac{6\sigma(1/2 - \rho)s_{\min}^{\text{LPC}}\varepsilon_g}{L_2}}, s_{\min}^{\text{LPC}}\varepsilon_g\right\} \varepsilon_g \\
 &\leq -\rho \min\left\{\frac{6\sigma(1/2 - \rho)s_{\min}^{\text{LPC}}/L_2}{\frac{3\Delta_H}{2L_2} + \sqrt{\frac{9\Delta_H^2}{4L_2^2} + \frac{6\sigma(1/2 - \rho)s_{\min}^{\text{LPC}}}{L_2}}}, s_{\min}^{\text{LPC}}\right\} \varepsilon_g^2 \\
 &= -\tilde{c}^{\text{LPC}} \varepsilon_g^2.
 \end{aligned}$$

On the fourth line we applied  $\|\tilde{\mathbf{p}}\| \geq s_{\min}^{\text{LPC}} \|\mathbf{g}\|$  and  $\|\mathbf{g}\| > \varepsilon_g$ , while in the fifth line we applied Lemma B.10 and  $\varepsilon_g < 1$ . In the final line we define

$$\tilde{c}^{\text{LPC}} \triangleq \rho \min \left\{ \frac{12\sigma(1/2 - \rho)s_{\min}^{\text{LPC}}}{3\Delta_H + \sqrt{9\Delta_H^2 + 24\sigma(1/2 - \rho)L_2s_{\min}^{\text{LPC}}}}, s_{\min}^{\text{LPC}} \right\}.$$

Finally, for the SPC case the line search condition (32) and  $\alpha \geq \min\{1, \alpha_2^*\}$  yields

$$\begin{aligned} f(\mathbf{x} + \alpha\tilde{\mathbf{p}}) - f(\mathbf{x}) &\leq -\rho\alpha \|\mathbf{g}\| \|\tilde{\mathbf{p}}\| \\ &\leq -\rho \min \{ \alpha_2^* \|\tilde{\mathbf{p}}\|, \|\tilde{\mathbf{p}}\| \} \|\mathbf{g}\| \\ &= -\rho \min \left\{ -\frac{3\Delta_H}{2L_2} + \sqrt{\frac{9\Delta_H^2}{4L_2^2} + \frac{6\sigma(1/2 - \rho) \|\tilde{\mathbf{p}}\|}{L_2}}, \|\tilde{\mathbf{p}}\| \right\} \|\mathbf{g}\| \\ &< -\rho \min \left\{ -\frac{3\Delta_H}{2L_2} + \sqrt{\frac{9\Delta_H^2}{4L_2^2} + \frac{6\sigma^2(1/2 - \rho)\varepsilon_g}{L_2\tilde{L}_1^2}}, \frac{\sigma}{\tilde{L}_1}\varepsilon_g \right\} \varepsilon_g \\ &\leq -\rho \min \left\{ \frac{6\sigma^2(1/2 - \rho)/(L_2\tilde{L}_1^2)}{\frac{3\Delta_H}{2L_2} + \sqrt{\frac{9\Delta_H^2}{4L_2^2} + \frac{6\sigma^2(1/2 - \rho)}{L_2\tilde{L}_1^2}}}, \frac{\sigma}{\tilde{L}_1} \right\} \varepsilon_g^2 \\ &= -\tilde{c}^{\text{SPC}} \varepsilon_g^2. \end{aligned}$$

We apply  $\|\tilde{\mathbf{p}}\| \geq (\sigma/\tilde{L}_1^2) \|\mathbf{g}\|$ , which follows from (31), and  $\|\mathbf{g}\| > \varepsilon_g$  in the fourth line, while in the fifth line we apply Lemma B.10. In the final line we define

$$\tilde{c}^{\text{SPC}} \triangleq \rho \min \left\{ \frac{12\sigma^2(1/2 - \rho)/\tilde{L}_1^2}{3\Delta_H + \sqrt{9\Delta_H^2 + 24\sigma^2(1/2 - \rho)L_2/\tilde{L}_1^2}}, \frac{\sigma}{\tilde{L}_1} \right\}.$$

The proof now proceeds similarly to the deterministic case. Let

$$K \triangleq \left\lceil \frac{f(\mathbf{x}_0) - f^*}{\min \{ \tilde{c}^{\text{NC}}, \tilde{c}^{\text{LPC}}, \tilde{c}^{\text{SPC}} \} \varepsilon_g^2} \right\rceil.$$

Suppose that  $\|\mathbf{g}_k\| \leq \varepsilon_g$  fails to hold for  $k = 0, \dots, K-1$ . We divide the iterations  $\mathcal{K} = \{0, \dots, K-1\}$  into a disjoint union  $\mathcal{K} = \mathcal{K}_{\text{NC}} \cup \mathcal{K}_{\text{LPC}} \cup \mathcal{K}_{\text{SPC}}$  where

$$\begin{aligned} \mathcal{K}_{\text{NC}} &= \left\{ k \in \mathcal{K} \mid \langle \mathbf{g}_k, \tilde{\mathbf{H}}_k \mathbf{g}_k \rangle < 0 \right\} \\ \mathcal{K}_{\text{LPC}} &= \left\{ k \in \mathcal{K} \mid 0 \leq \langle \mathbf{g}_k, \tilde{\mathbf{H}}_k \mathbf{g}_k \rangle \leq \sigma \|\mathbf{g}_k\|^2 \right\} \\ \mathcal{K}_{\text{SPC}} &= \left\{ k \in \mathcal{K} \mid \langle \mathbf{g}_k, \tilde{\mathbf{H}}_k \mathbf{g}_k \rangle > \sigma \|\mathbf{g}_k\|^2 \right\}. \end{aligned}$$

Applying a telescoping sum and the lower bounds on function decrease in each case, we have

$$\begin{aligned} f(\mathbf{x}_0) - f(\mathbf{x}_K) &= \sum_{i=0}^{K-1} f(\mathbf{x}_i) - f(\mathbf{x}_{i+1}) \\ &= \sum_{k \in \mathcal{K}_{\text{NC}}} f(\mathbf{x}_k) - f(\mathbf{x}_{k+1}) + \sum_{k \in \mathcal{K}_{\text{LPC}}} f(\mathbf{x}_k) - f(\mathbf{x}_{k+1}) + \sum_{k \in \mathcal{K}_{\text{SPC}}} f(\mathbf{x}_k) - f(\mathbf{x}_{k+1}) \\ &> |\mathcal{K}_{\text{NC}}| \tilde{c}^{\text{NC}} \varepsilon_g^2 + |\mathcal{K}_{\text{LPC}}| \tilde{c}^{\text{LPC}} \varepsilon_g^2 + |\mathcal{K}_{\text{SPC}}| \tilde{c}^{\text{SPC}} \varepsilon_g^2 \\ &\geq (|\mathcal{K}_{\text{NC}}| + |\mathcal{K}_{\text{LPC}}| + |\mathcal{K}_{\text{SPC}}|) \min \{ \tilde{c}^{\text{NC}}, \tilde{c}^{\text{LPC}}, \tilde{c}^{\text{SPC}} \} \varepsilon_g^2 \\ &= K \min \{ \tilde{c}^{\text{NC}}, \tilde{c}^{\text{LPC}}, \tilde{c}^{\text{SPC}} \} \varepsilon_g^2 \\ &\geq f(\mathbf{x}_0) - f^*, \end{aligned}$$

which implies  $f(\mathbf{x}_K) < f^*$ , a contradiction.  $\square$

**Remark on Proposition 3.12** Notably, Proposition 3.12 does not require an explicit bound on the Hessian error,  $\Delta_H$ . However, as we now demonstrate, the per iteration dependence on  $\varepsilon_g$  can be improved (relative to the worst case) for SPC steps if we impose a bound on  $\Delta_H$ . In particular, we stipulate that, for  $\theta \in [0, 1)$ , the Hessian error tolerance satisfies

$$\Delta_H \leq 2\theta\sigma(1/2 - \rho). \quad (36)$$

Consider then a “large  $\tilde{\mathbf{p}}$ ” setting (similar to Proposition 3.2) defined by

$$\|\tilde{\mathbf{p}}\| \geq \frac{6\sigma(1/2 - \rho) - 3\Delta_H}{L_2} = \frac{6\sigma(1/2 - \rho)}{L_2} - \frac{3\Delta_H}{L_2}.$$

Note that the lower bound on  $\tilde{\mathbf{p}}$  is nontrivial because of the bound in (36). Rearranging and subbing to the step size acceptance tolerance for the SPC case,  $\alpha_2^*$ , we have

$$\begin{aligned} \alpha_2^* &= -\frac{3\Delta_H}{2L_2\|\tilde{\mathbf{p}}\|} + \sqrt{\frac{9\Delta_H^2}{4L_2^2\|\tilde{\mathbf{p}}\|^2} + \frac{6\sigma(1/2 - \rho)}{L_2\|\tilde{\mathbf{p}}\|}} \\ &\leq -\frac{3\Delta_H}{2L_2\|\tilde{\mathbf{p}}\|} + \sqrt{\frac{9\Delta_H^2}{4L_2^2\|\tilde{\mathbf{p}}\|^2} + \frac{\|\tilde{\mathbf{p}}\| + \frac{3\Delta_H}{L_2}}{\|\tilde{\mathbf{p}}\|}} \\ &= -\frac{3\Delta_H}{2L_2\|\tilde{\mathbf{p}}\|} + \sqrt{1 + \frac{9\Delta_H^2}{4L_2^2\|\tilde{\mathbf{p}}\|^2} + \frac{3\Delta_H}{L_2\|\tilde{\mathbf{p}}\|}} \\ &= -\frac{3\Delta_H}{2L_2\|\tilde{\mathbf{p}}\|} + \sqrt{\left(1 + \frac{3\Delta_H}{2L_2\|\tilde{\mathbf{p}}\|}\right)^2} \\ &= 1. \end{aligned}$$

Therefore, for large  $\tilde{\mathbf{p}}$  the largest step size that satisfies (32), must also satisfy  $\alpha \geq \alpha_2^*$ . Additionally, applying (36) to the lower bound on  $\|\tilde{\mathbf{p}}\|$  we obtain

$$\|\tilde{\mathbf{p}}\| \geq \frac{6\sigma(1/2 - \rho) - 3\Delta_H}{L_2} \geq \frac{6\sigma(1 - \theta)(1/2 - \rho)}{L_2}.$$

By combining the line search condition (32),  $\alpha \geq \alpha_2^*$ , (30), the SPC curvature test and the lower bound on  $\|\tilde{\mathbf{p}}\|$  we have

$$\begin{aligned} f(\mathbf{x} + \alpha\tilde{\mathbf{p}}) - f(\mathbf{x}) &\leq \alpha\rho\langle\tilde{\mathbf{p}}, \mathbf{g}\rangle \\ &\leq -\alpha_2^*\rho\langle\tilde{\mathbf{p}}, \tilde{\mathbf{H}}\tilde{\mathbf{p}}\rangle \\ &\leq -\rho\left(-\frac{3\Delta_H}{2L_2\|\tilde{\mathbf{p}}\|} + \sqrt{\frac{9\Delta_H^2}{4L_2^2\|\tilde{\mathbf{p}}\|^2} + \frac{6\sigma(1/2 - \rho)}{L_2\|\tilde{\mathbf{p}}\|}}\right)\sigma\|\tilde{\mathbf{p}}\|^2 \\ &\leq -\sigma\rho\left(-\frac{3\Delta_H}{2L_2} + \sqrt{\frac{9\Delta_H^2}{4L_2^2} + \frac{6\sigma(1/2 - \rho)\|\tilde{\mathbf{p}}\|}{L_2}}\right)\|\tilde{\mathbf{p}}\| \\ &\leq -\sigma\rho\left(-\frac{3\Delta_H}{2L_2} + \sqrt{\frac{9\Delta_H^2}{4L_2^2} + \frac{36\sigma^2(1/2 - \rho)^2(1 - \theta)}{L_2^2}}\right)\left(\frac{6\sigma(1 - \theta)(1/2 - \rho)}{L_2}\right) \\ &= -\sigma\rho\left(\frac{72\sigma^2(1/2 - \rho)^2(1 - \theta)/L_2}{3\Delta_H + \sqrt{9\Delta_H^2 + 144\sigma^2(1/2 - \rho)^2(1 - \theta)}}\right)\left(\frac{6\sigma(1 - \theta)(1/2 - \rho)}{L_2}\right) \\ &= -\frac{\sigma\rho}{L_2^2}\left(\frac{432\sigma^3(1/2 - \rho)^3(1 - \theta)^2}{3\Delta_H + \sqrt{9\Delta_H^2 + 144\sigma^2(1/2 - \rho)^2(1 - \theta)}}\right). \quad (37) \end{aligned}$$

This bound suggests that, analogously to the “large  $\mathbf{p}$ ” case for the exact Hessian, a better dependence on  $\varepsilon_g$  is obtained when  $\tilde{\mathbf{p}}$  is large and  $\Delta_H$  is controlled. In fact, when  $\theta = 0$  we have  $\Delta_H = 0$  and (37) matches the “large  $\mathbf{p}$ ” exact case. In conclusion, despite the worst case headline rate, in some cases a better dependence on  $\varepsilon_g$  may be obtained for certain steps if  $\Delta_H$  is controlled.

### B.7. Sub-sampled Hessian Error Bound

**Lemma B.11** (Hessian Sub-sampling). *Consider the finite sum objective*

$$f(\mathbf{x}) = \frac{1}{n} \sum_{i=1}^n f_i(\mathbf{x}).$$

Suppose that there exists  $0 \leq L_1^{\max} < \infty$  such that for all  $\mathbf{x} \in \mathbb{R}^d$  we have  $\max_{i=1, \dots, n} \|\mathbf{H}_i \mathbf{g}\| \leq L_1^{\max} \|\mathbf{g}\|$ . Let  $\delta \in (0, 1)$  and  $\tilde{\mathbf{H}}$  be as in (12). Then for any  $\Delta_H \geq 0$  and  $\mathbf{x} \in \mathbb{R}^d$  we have

$$\mathbb{P} \left( \left\| (\tilde{\mathbf{H}} - \mathbf{H}) \mathbf{g} \right\| \leq \Delta_H \|\mathbf{g}\| \right) \geq 1 - \delta,$$

if

$$|\mathcal{I}_H| \geq \frac{(L_1^{\max})^2 \left(1 + \sqrt{8 \log(1/\delta)}\right)^2}{\Delta_H^2}.$$

*Proof.* The result proceeds similarly to Roosta & Mahoney (2019, Lemma 3). First we write  $\mathbf{H}\mathbf{g} = \mathbf{A}\mathbf{B}$  where

$$\mathbf{A} = [\mathbf{H}_1 \mathbf{g}, \dots, \mathbf{H}_n \mathbf{g}] \in \mathbb{R}^{d \times n}, \quad \mathbf{B} = [1/n, \dots, 1/n]^\top \in \mathbb{R}^n.$$

We would like to relate this matrix product to the subsampled alternative. To do this, take the minibatch,  $\mathcal{I}_H$ , and form  $\tilde{\mathbf{A}} \in \mathbb{R}^{d \times |\mathcal{I}_H|}$ , using the columns of  $\mathbf{A}$  corresponding to  $\mathcal{I}_H$ , rescaled by  $\sqrt{n/|\mathcal{I}_H|}$ . Similarly, form  $\tilde{\mathbf{B}} \in \mathbb{R}^{|\mathcal{I}_H|}$ , using the rows of  $\mathbf{B}$  corresponding to  $\mathcal{I}_H$ , rescaled by  $\sqrt{n/|\mathcal{I}_H|}$ . Clearly,

$$\tilde{\mathbf{A}}\tilde{\mathbf{B}} = \frac{n}{|\mathcal{I}_H|} \sum_{i \in \mathcal{I}_H} \frac{1}{n} \mathbf{H}_i \mathbf{g} = \tilde{\mathbf{H}}\mathbf{g}.$$

Applying Drineas et al. (2006, Lemma 11) allows us to relate  $\mathbf{A}\mathbf{B}$  to  $\tilde{\mathbf{A}}\tilde{\mathbf{B}}$ . In particular, with probability at least  $1 - \delta$ , we have

$$\begin{aligned} \left\| \mathbf{H}\mathbf{g} - \tilde{\mathbf{H}}\mathbf{g} \right\| &= \left\| \mathbf{A}\mathbf{B} - \tilde{\mathbf{A}}\tilde{\mathbf{B}} \right\| \leq \sqrt{\frac{n}{|\mathcal{I}_H|} \sum_{i=1}^n \|\mathbf{A}_i\|^2 \|\mathbf{B}_i\|^2} + \frac{n}{\sqrt{|\mathcal{I}_H|}} \sqrt{8 \log(1/\delta)} \max_{i=1, \dots, n} \|\mathbf{A}_i\| \|\mathbf{B}_i\| \\ &\leq \sqrt{\frac{1}{n|\mathcal{I}_H|} \sum_{i=1}^n \|\mathbf{H}_i \mathbf{g}\|^2} + \frac{n}{\sqrt{|\mathcal{I}_H|}} \sqrt{8 \log(1/\delta)} \max_{i=1, \dots, n} \|\mathbf{H}_i \mathbf{g}\| / n \\ &\leq \sqrt{\frac{1}{|\mathcal{I}_H|} (L_1^{\max})^2 \|\mathbf{g}\|^2} + \sqrt{\frac{8 \log(1/\delta)}{|\mathcal{I}_H|}} L_1^{\max} \|\mathbf{g}\| \\ &\leq \frac{1}{\sqrt{|\mathcal{I}_H|}} \left(1 + \sqrt{8 \log(1/\delta)}\right) L_1^{\max} \|\mathbf{g}\|. \end{aligned}$$

Finally, we see that

$$|\mathcal{I}_H| \geq \frac{(L_1^{\max})^2 \left(1 + \sqrt{8 \log(1/\delta)}\right)^2}{\Delta_H^2} \implies \frac{1}{\sqrt{|\mathcal{I}_H|}} \left(1 + \sqrt{8 \log(1/\delta)}\right) L_1^{\max} \leq \Delta_H.$$

□

As a result of Lemma B.11 it is clear that Assumption 3.9 is satisfied with high probability as, by the Cauchy-Schwarz inequality, we have

$$\left| \left\langle \mathbf{g}, (\mathbf{H} - \tilde{\mathbf{H}})\mathbf{g} \right\rangle \right| \leq \|\mathbf{g}\| \left\| (\mathbf{H} - \tilde{\mathbf{H}})\mathbf{g} \right\|.$$

## C. Miscellaneous Scaling Properties

**MR Scaling Tighter Lower Bound** Recall from Lemma B.3 that if  $\|\mathbf{H}\mathbf{g}\| \leq L_1 \|\mathbf{g}\|$  for some  $L_1$  (see Assumption 3.3) then the CG, MR and GM scalings satisfy a lower bound in terms of the gradient norm. Notably, the MR scaling lower bound is weaker by a factor of  $\sigma/L_1$ , in comparison with the CG and GM. In the following lemma we show that this lower bound can be tightened to match the CG and GM case if the Hessian spectrum is positive and bounded.

**Lemma C.1.** *If the Hessian satisfies  $0 \preceq \mathbf{H} \preceq M\mathbf{I}$  and  $\|\mathbf{H}\mathbf{g}\| > 0$  then*

$$s^{\text{MR}} \geq 1/M.$$

*Proof.* We utilise the fact that  $s^{\text{MR}}$  is a Rayleigh quotient of  $\mathbf{H}^\dagger$ . Suppose that  $\mathbf{H}$  has  $\psi_+$  nonzero eigenvalues ( $\|\mathbf{H}\mathbf{g}\| > 0$  implies  $\psi_+ > 0$ ) given by  $0 < \lambda_1 < \lambda_2 \leq \dots \leq \lambda_{\psi_+} \leq M$ . The corresponding nonzero eigenvalues of  $\mathbf{H}^\dagger$  are given by  $1/\lambda_{\psi_+} \leq \dots \leq 1/\lambda_1$ . Since  $\mathbf{H}\mathbf{g} \in \text{Range}(\mathbf{H})$  and is therefore orthogonal to  $\text{Null}(\mathbf{H})$  we have

$$s^{\text{MR}} = \frac{\langle \mathbf{g}, \mathbf{H}\mathbf{g} \rangle}{\|\mathbf{H}\mathbf{g}\|^2} = \frac{\langle \mathbf{H}\mathbf{g}, \mathbf{H}^\dagger \mathbf{H}\mathbf{g} \rangle}{\|\mathbf{H}\mathbf{g}\|^2} \geq \frac{1}{\lambda_{\psi_+}} \frac{\|\mathbf{H}\mathbf{g}\|^2}{\|\mathbf{H}\mathbf{g}\|^2} \geq \frac{1}{M}.$$

□

The requirement that  $\|\mathbf{H}\mathbf{g}\| > 0$  is not stringent since the positive curvature test  $\langle \mathbf{g}, \mathbf{H}\mathbf{g} \rangle > 0$  implies  $\mathbf{H}\mathbf{g} \neq \mathbf{0}$ .

## D. Additional Numerical Results

### D.1. Oracle Calls as Complexity Measure

Following the typical convention in the optimization literature, in all our experiments, we plot the objective value against the total number of oracle calls for function, gradient, and Hessian-vector product evaluations, which allows for a fair comparison between methods with a differing per-iteration computational costs. We adopt this approach because the measurement of “wall-clock” time can be heavily dependent on specific implementation details and computational platform. In contrast, counting the number of equivalent function evaluations, as an implementation and system independent unit of complexity is more appropriate and fair. More specifically, upon evaluating the function, computing its gradient is equivalent to one additional function evaluation, and computing a Hessian-vector product requires two additional function evaluations compared to a gradient evaluation (Pearlmutter, 1994). For example, in neural networks, for given data at the input layer, evaluation of network’s output, i.e., function evaluation, involves one forward propagation. The corresponding gradient is computed by performing one additional backward propagation. After computing the gradient, an additional forward followed by a backward propagation give the corresponding Hessian-vector product (Goodfellow et al., 2016; Blondel & Roulet, 2024).

### D.2. Multi-class Logistic Regression

Consider a set of data items  $\mathcal{D} = \{\mathbf{a}_i, b_i\}_{i=1}^n \subset \mathbb{R}^d \times \{1, \dots, C\}$ . Denote the weights of each class as  $\mathbf{x}_1, \dots, \mathbf{x}_C$  and define  $\mathbf{x} = [\mathbf{x}_1, \dots, \mathbf{x}_{C-1}]$ . We are free to take  $\mathbf{x}_C = \mathbf{0}$  as class  $C$  is identifiable from the weights of the other classes. The objective,  $f$ , is given by

$$f(\mathbf{x}) = \frac{1}{n} \sum_{i=1}^n \sum_{c=1}^{C-1} -\mathbf{1}(b_i = c) \log(\text{softmax}(\mathbf{x}_c, \mathbf{a}_i)) + \frac{\lambda}{2} \|\mathbf{x}\|^2, \quad (38)$$

where  $\mathbf{1}(\cdot)$  is the indicator function and

$$\text{softmax}(\mathbf{x}_c, \mathbf{a}_i) = \frac{\exp(\langle \mathbf{x}_c, \mathbf{a}_i \rangle)}{\sum_{c=1}^C \exp(\langle \mathbf{x}_c, \mathbf{a}_i \rangle)}.$$

In our experiments a bias parameter is included in the weights for each class. We set the regularization parameter to  $\lambda = 10^{-3}$  and initialize by setting  $\mathbf{x}_0 = \mathbf{0}$ . We run all methods until a maximum of  $10^5$  oracle calls or until  $\|\mathbf{g}_k\| \leq 10^{-4}$ .

Note that the spectrum of the Hessian of (38) can be bounded as

$$\lambda \mathbf{I} \preceq \nabla^2 f(\mathbf{x}) \preceq \left( \frac{C-1}{4n} \|\mathbf{A}\|^2 + \lambda \right) \mathbf{I}, \quad (39)$$

which allows us to estimate the strong convexity parameter and Lipschitz constant of (38) as

$$\mu_{\text{approx}} \triangleq \lambda, \quad L_{\text{approx}} \triangleq \frac{C-1}{4n} \|\mathbf{A}\|^2 + \lambda.$$

**Parameter Settings** For the scaled gradient methods, we compare between CG, MR, GM, MRCG, CGMR, GMCG, GMMR and CGMR scalings. We set  $\sigma = 0$  as (38) is  $\mu$ -strongly convex (i.e., curvature along the gradient is already lower bounded). For the line search, we apply a backtracking procedure (Algorithm 3) with  $\theta = 0.5$  and  $\rho = 10^{-4}$ , which is a common choice in the literature.

For line search gradient descent, we apply a backtracking procedure (Algorithm 3) based on the Amijo condition (7) with  $\mathbf{p} = -\mathbf{g}$ ,  $\theta = 0.5$ ,  $\alpha_0 = 1$  and  $\rho = 10^{-4}$ . For fixed step size gradient descent we use a step size of  $\alpha = 1/L_{\text{approx}}$ . In terms of the momentum methods, we consider updates of the form

$$\begin{cases} \mathbf{v}_{k+1} = \beta \mathbf{v}_k - \alpha \mathbf{g}_k \\ \mathbf{x}_{k+1} = \begin{cases} \mathbf{x}_k + \mathbf{v}_{k+1} & \text{if Heavy ball.} \\ \mathbf{x}_k - \alpha \mathbf{g}_k + \beta \mathbf{v}_{k+1} & \text{if Nesterov.} \end{cases} \end{cases} \quad (40)$$

where  $\alpha$  is a ‘step size’ parameter and  $\beta$  is a momentum parameter. For  $\mu$ -strongly convex,  $L_{\mathbf{g}}$ -smooth problems the parameters for the Heavy ball momentum (Polyak, 1987) can be set as

$$\alpha = \frac{4}{(\sqrt{L_{\mathbf{g}}} + \sqrt{\mu})^2}, \quad \beta = \left( \frac{\sqrt{L_{\mathbf{g}}} - \sqrt{\mu}}{\sqrt{L_{\mathbf{g}}} + \sqrt{\mu}} \right)^2.$$

While for Nesterov acceleration (Nesterov, 2004) the step size and momentum parameter can be set as

$$\alpha = \frac{1}{L_{\mathbf{g}}}, \quad \beta = \frac{1 - \sqrt{L_{\mathbf{g}}/\mu}}{1 + \sqrt{L_{\mathbf{g}}/\mu}}.$$

In our experiments we use these settings with  $\mu_{\text{approx}}$  and  $L_{\text{approx}}$  taking the place of  $\mu$  and  $L_{\mathbf{g}}$ , respectively. Finally, for Adam (Kingma, 2014) we use standard values of  $\beta_1 = 0.9$ ,  $\beta_2 = 0.999$  and  $\epsilon = 10^{-8}$  and then tune the step size parameter by selecting the largest step size in power of 10 increments with stable convergence along the optimization trajectory. This procedure resulted in a step size of  $\alpha = 10^{-3}$ .

**Additional Results** We now present some additional numerical results for the multi-class logistic regression problem. In Figure 4 we evaluate the performance of each of the scaled gradient methods. We see that CGMR and MRCG (which differ by whether they start on the CG or MR scaling, respectively) perform quite similarly outside of the initial convergence phase and handily outperform the other methods.

In Figure 5 and Figure 6 we see a breakdown of the performance of the ‘CG’ and ‘MR’ scalings, respectively. Firstly, in panel (c) for each method, we see that the unit step size is accepted by the line search at each iteration, similarly to MRCG. For the MR scaling (Figure 6) we plot the gradient norm in the (a) panel, from which we see that the MR method produces a monotonic decrease in the gradient norm at each iteration with a unit step size; indicating the results from Theorem 3.8 can hold over a wide portion of the optimization landscape. This is despite the line search targeting the function value, rather than the gradient norm. In panel (b) of Figure 5 and Figure 6 we see that the oscillating behavior is observed in the scaling values. However, comparing with Figure 1, it is clear that this oscillation is over a smaller range of values (particularly for MR scaling) than the alternating MRCG scaling. This indicates that the alternation between MR and CG scalings is key to obtaining large scaling values and, in light of Theorem 3.8, corresponding rapid convergence.

Finally, in Figure 7 we plot the objective value against wall-clock time we see that results largely conform with oracle calls.

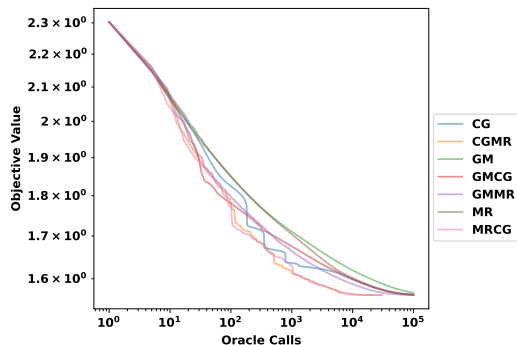


Figure 4. Comparison between scaling method performance for multiclass logistic regression on CIFAR10.

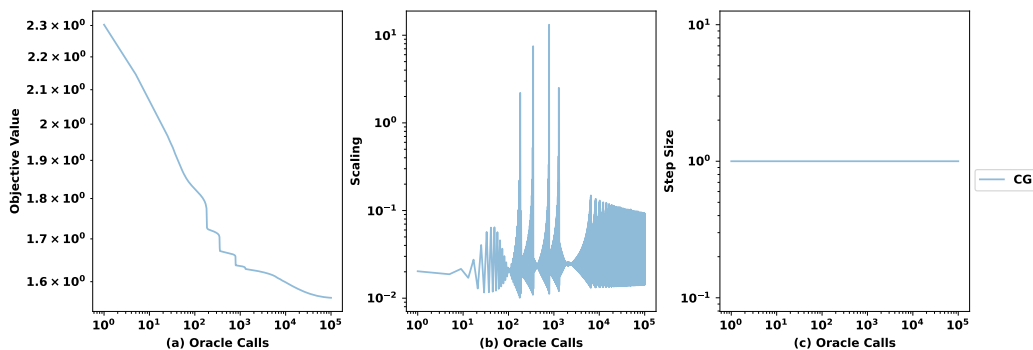


Figure 5. Performance of the CG scaling on the multi-class logistic regression problem on CIFAR10. (a) The objective function. (b) The scaling selected by the CG method. (c) The step size selected by line search.

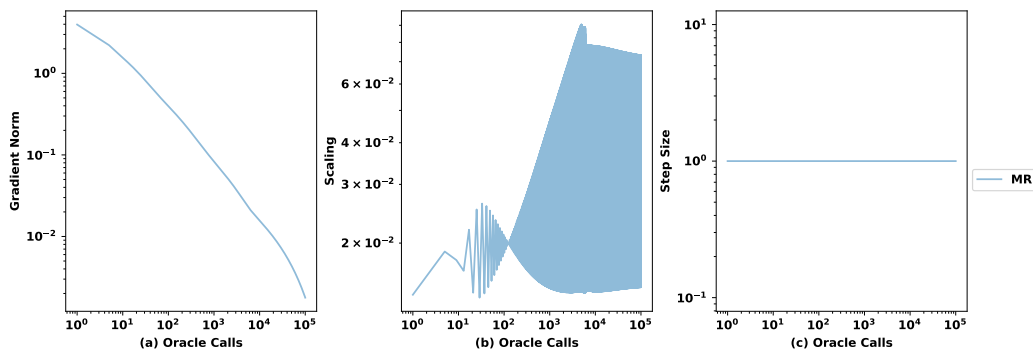


Figure 6. Performance of the MR scaling on the multi-class logistic regression problem on CIFAR10. (a) The gradient norm. (b) The scaling selected by the MR method. (c) The step size selected by line search.

### D.3. MLP

Let  $\mathbf{h}(\mathbf{x}; \cdot)$  denote a two layer MLP with 100 hidden units per layer with GeLU (Hendrycks & Gimpel, 2016) activations and  $C$  output layers, with parameters  $\mathbf{x}$ . The objective for our experiment is the function

$$f(\mathbf{x}) = \frac{1}{n} \sum_{i=1}^n \text{CrossEntropy}(\mathbf{h}(\mathbf{x}; \mathbf{a}_i), b_i) + \frac{\lambda}{2} \|\mathbf{x}\|^2, \quad (41)$$

where  $\text{CrossEntropy}(\cdot, \cdot)$  is the cross-entropy loss between the predictions of the MLP and the true labels and  $\lambda$  is a  $\ell_2$  regularization (or weight decay) parameter. In our experiments the regularization parameter was set to  $\lambda = 10^{-3}$  and the parameters were initialised with the PyTorch default, that is, the weights for each layer are drawn from  $U(-\sqrt{k}, \sqrt{k})$  where  $k = 1/(\#\text{num inputs to the layer})$ . We run all methods until a maximum of  $10^5$  oracle calls or until  $\|\mathbf{g}_k\| \leq 10^{-4}$ .



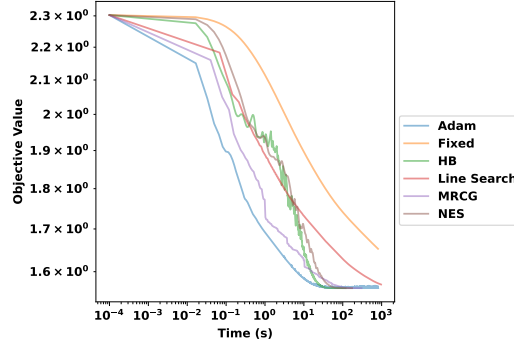


Figure 7. Wall-clock time for multi-class logistic regression on the CIFAR10 dataset.  $10^{-4}$  has been added to all times for plotting purposes.

**Parameter Settings** For the scaled methods we utilize the same set of scalings at the logistic regression case. We set  $\sigma = 10^{-6}$  and utilize fixed scalings given by  $s^{\text{LPC}} = s^{\text{NC}} = 1$ . For the line search, we set  $\rho = 10^{-4}$  and we use  $\theta = 0.5$  as the scale factor for back and forward-tracking. For vanilla gradient descent with line search, we apply the same parameters as for the logistic regression experiment. Since (41) is nonconvex and there is no closed expression for the gradient Lipschitz constant, we set the parameters for the remaining methods by a tuning procedure. Specifically, for fixed step size gradient descent we tune the step size parameter by reducing the step size (with power of 10 increments) until stable convergence is achieved (i.e. no divergence or large scale oscillation) along optimization trajectory. For momentum methods (40) we fix  $\beta = 0.9$  and tune the step size parameter by a similar procedure. For Adam we use  $\beta_1 = 0.9$ ,  $\beta_2 = 0.999$  and  $\epsilon = 10^{-8}$  and, again, tune the step size parameter in a similar manner to the fixed step size case. The resulting learning rate parameters are summarized in Table 1

Method	Learning Rate
Fixed	$10^{-2}$
Adam	$10^{-5}$
HB	$10^{-3}$
NES	$10^{-3}$

Table 1. Tuned learning rates for MLP model on FashionMNIST

**Additional Results** We report some additional results for the MLP model on FashionMNIST dataset. In Figure 8 we compare the performance of each of the scalings on the problem. Again, we see that the alternating scalings ‘‘CGMR’’ and ‘‘MRCG’’ perform the best.

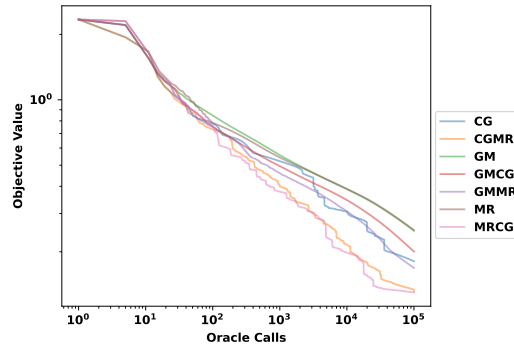


Figure 8. Comparison between scaling methods for MLP on FashionMNIST dataset.

In Figure 9 and Figure 10 we consider the performance of the CG and MR methods, respectively. For the MR scaling (Figure 10) we see that the unit step length is accepted at each iteration except for the iteration where NC is detected. At this

iteration the forward tracking line search kicks in and a larger step size is selected. Similar, to the logistic regression case, in panel (a) of Figure 10 we see that the gradient norm is monotonic, except for iteration where NC is detected, reinforcing the results in Theorem 3.8. On the other hand, for the CG scaling (Figure 9) NC is detected at a single iteration, where the forward tracking line search selects a larger step size. Also a handful of SPC iterations require a small adjustment to the step size from the line search, however in the terminal phase of the algorithm the unit step size is acceptable, consistent with Proposition 3.2. No LPC directions are detected for either the MR or CG scaling.

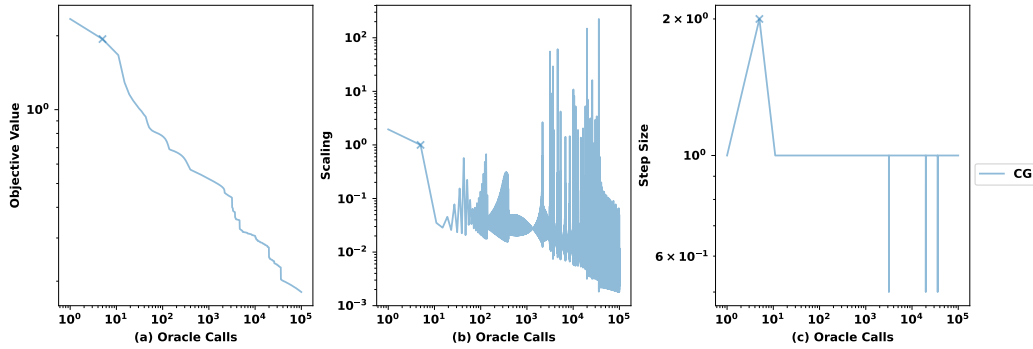


Figure 9. Performance of the CG scaling for the MLP on the FashionMNIST dataset. (a) The objective function. (b) The scaling selected by the CG method. (c) The step size selected by line search. Crosses indicate iterations where negative curvature is detected.

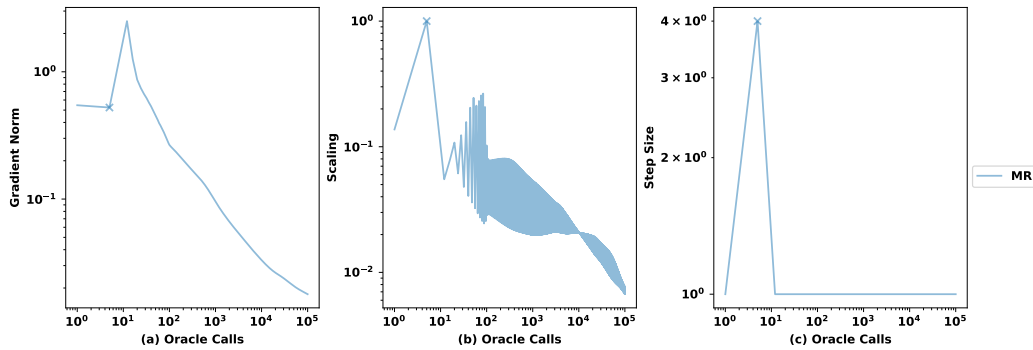


Figure 10. Performance of the MR scaling for the MLP on the FashionMNIST dataset. (a) The gradient norm. (b) The scaling selected by the MR method. (c) The step size selected by line search. Crosses indicate iterations where negative curvature is detected.

In Figure 11 we report our results from Figure 2 in terms of wall-clock time. We see that the results are largely unchanged.

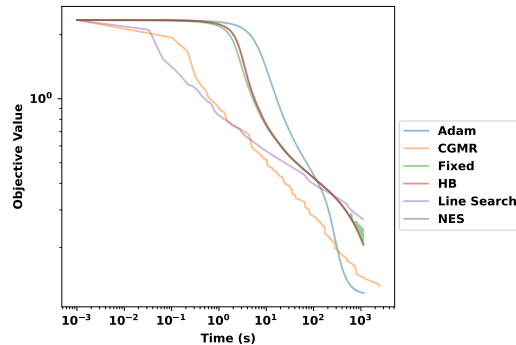


Figure 11. Wall-clock time results for MLP on the FashionMNIST dataset (Xiao et al., 2017).  $10^{-3}$  has been added to all times for plotting purposes.

#### D.4. Resnet

Let  $\mathbf{h}(\mathbf{x}, \cdot)$  denote a depth 18 ResNet (He et al., 2016) with parameters  $\mathbf{x}$ . The objective for our experiment is the function

$$f(\mathbf{x}) = \frac{1}{n} \sum_{i=1}^n \text{CrossEntropy}(\mathbf{h}(\mathbf{x}; \mathbf{a}_i), b_i) + \frac{\lambda}{2} \|\mathbf{x}\|^2, \tag{42}$$

where  $\text{CrossEntropy}(\cdot, \cdot)$  is the cross-entropy loss between the predictions of the network and the true labels and  $\lambda$  is an  $\ell_2$  regularization parameter. We specifically consider off-the-shelf ResNet18 implementation from PyTorch<sup>8</sup> with two modifications. Firstly, we replace all ReLU activations with GeLU (Hendrycks & Gimpel, 2016) to ensure twice differentiability. The second modification is replacing the BatchNorm (Ioffe & Szegedy, 2015) layers with LayerNorm (Ba et al., 2016). This modification has previously been considered in (Wu & He, 2018). We utilize the “160px” version of the Imagenette dataset (Howard, 2019), which is available from PyTorch (Paszke et al., 2019). The Imagenette is a 10 class, subset of the full Imagenet dataset (Deng et al., 2009). We process the data by normalizing per channel using Imagenet (Deng et al., 2009) statistics followed by resizing the images to  $32 \times 32$ .

In our experiments we set  $\lambda = 10^{-5}$  and use the default initialization for the PyTorch ResNet model. All experiments are run until a maximum of  $10^4$  oracle calls or  $\|\mathbf{g}_k\| \leq 10^{-4}$ .

**Parameter Settings** Given the results of the previous experiments, we chose to focus on the MRCG, MR and CG as our scaling methods in this experiment. Additionally, as noted in the main body we disabled the line search and simply used a fixed step size of  $\alpha = 1$ . We set  $\sigma = 10^{-6}$  and  $s^{\text{NC}} = s^{\text{LPC}} = 1$ . Although, we never encounter NC or LPC directions throughout iterations, it could be beneficial to retain the line search for NC and LPC directions as the scaling selections for these cases are arbitrary.

For vanilla gradient descent with line search, we apply a backtracking search procedure (Algorithm 3) based on the Amijo condition (7) with  $\mathbf{p} = -\mathbf{g}$ ,  $\theta = 0.5$ ,  $\alpha_0 = 1$  and  $\rho = 0$ . This choice of  $\rho$  was made for numerical stability purposes as it simply forces monotonicity of the function value, rather than “sufficient decrease”. We set the learning rates for all other methods by tuning over a grid of candidate values (unlike the MLP and logistic regression experiments, larger learning weren’t necessarily better). We give the search grid as well as the selected learning rate in Table 2. All other hyperparameters we left the same as the MLP setup; see Appendix D.3.

Method	Grid	Learning Rate
Fixed	$\{10^0, 10^{-1}, 10^{-2}, 10^{-3}\}$	$10^{-1}$
Adam	$\{10^{-2}, 10^{-3}, 10^{-4}, 10^{-5}\}$	$10^{-3}$
HB	$\{10^{-1}, 10^{-2}, 10^{-3}\}$	$10^{-2}$
NES	$\{10^{-1}, 10^{-2}, 10^{-3}\}$	$10^{-2}$

Table 2. Learning rate tuning for ResNet18 model on Imagenette.

**Additional Results** We now collect the additional results from our ResNet18 experiments. In Figure 12 we see that, similar to the previous two experiments, alternating MRCG scaling performs significantly better than either MR or CG on their own.

In Figure 13 and Figure 14 we consider the CG and MR scalings in particular. Inspecting panel (b) of both figures and comparing with Figure 3, we see that the alternating MRCG scaling is capable of producing significantly larger scaling values, which could explain the faster convergence of the alternating scaling. In panel (a) of Figure 14 we plot the gradient norm of the objective, we see that, similar to the MLP and logistic regression example, the MR scaling produces monotonic decrease in the gradient norm with the unit step size. This result is consistent with Theorem 3.8.

In Figure 15 we plot the results from Figure 3 against wall-clock time. We see that the results roughly conform with the oracle call results.

<sup>8</sup>Available [here](#).

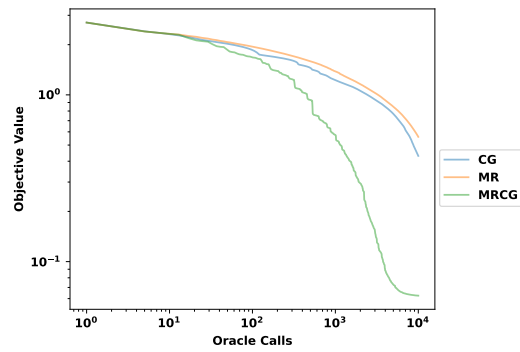


Figure 12. Comparison of scaling method performance on for the ResNet18 model on the Imagenette dataset

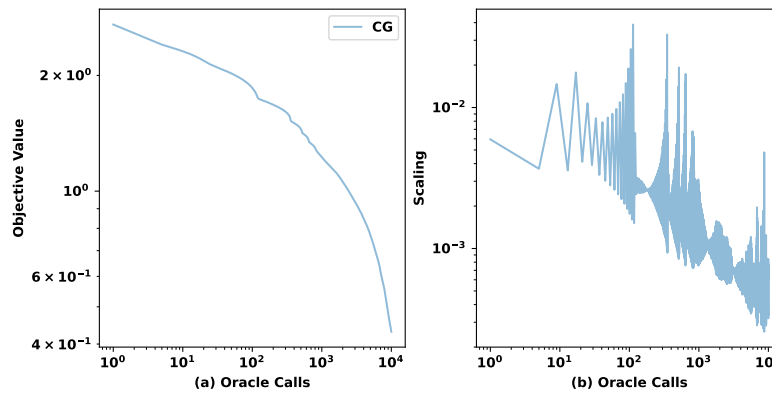


Figure 13. Performance of the CG scaling for the ResNet18 model on Imagenette dataset. (a) The objective function. (b) The scaling selected by the CG method.

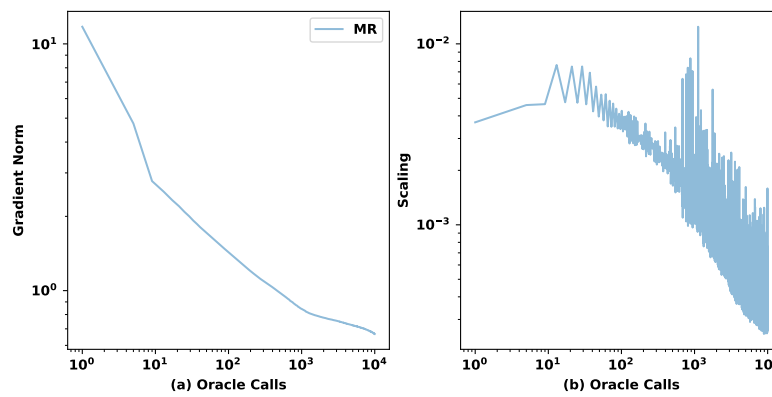


Figure 14. Performance of the MR scaling for the ResNet18 model on Imagenette dataset. (a) The objective function. (b) The scaling selected by the MR method.

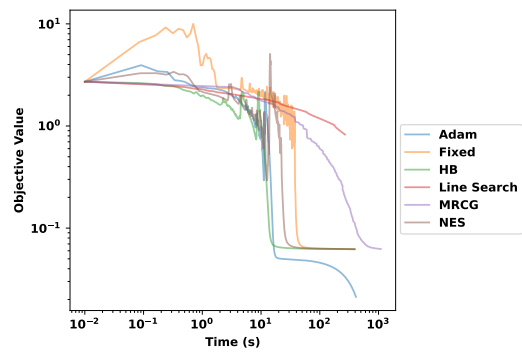


Figure 15. Wall-clock time results for the ResNet18 model on Imagenette dataset.  $10^{-2}$  has been added to all times for plotting purposes.